NASA CR-156884

(NASA-CR-156884) A UNIFIED THERMAL AND VERTICAL TRAJECTORY MODEL FOR THE PREDICTION OF HIGH ALTITUDE BALLOON PERFORMANCE Final Report (Texas A&M Univ.) 90 p HC A05/MF A01 CSCL 01A G3/02

N82-16048

Unclas
07719

TEXAS A&M UNIVERSITY

A UNIFIED THERMAL AND VERTICAL TRAJECTORY MODEL FOR THE PREDICTION OF HIGH ALTITUDE BALLOON PERFORMANCE

LELAND A. CARLSON
WALTER J. HORN
AEROSPACE ENGINEERING DEPARTMENT
TEXAS A&M UNIVERSITY
COLLEGE STATION, TEXAS 77843

TAMRF REP. NO. 4217-81-01

JUNE 1981

TEXAS ENGINEERING EXPERIMENT STATION

A UNIFIED THERMAL AND VERTICAL TRAJECTORY MODEL FOR THE PREDICTION OF HIGH ALTITUDE BALLOON PERFORMANCE

LELAND A. CARLSON

WALTER J. HORN

AEROSPACE ENGINEERING DEPARTMENT
TEXAS A&M UNIVERSITY
COLLEGE STATION, TEXAS 77843

TAMRF REPT. NO. 4217-81-01

JUNE 1981

A UNIFIED THERMAL AND VERTICAL TRAJECTORY MODEL FOR THE PREDICTION OF HIGH ALTITUDE BALLOON PERFORMANCE

Leland A. Carlson

Walter J. Horn

SUMMARY

A new computer model for the prediction of the trajectory and thermal behavior of zero-pressure high altitude balloon has been developed. In accord with flight data, the model permits radiative emission and absorption of the lifting gas and daytime gas temperatures above that of the balloon film. It also includes ballasting, venting, and valving. Predictions obtained with the model are compared with flight data from several flights and newly discovered features are discussed.

TABLE OF CONTENTS

NOMENCLATURE

A - Cross sectional area of balloon

c_f - Specific heat of the balloon film

c_{pg} - Specific heat of the balloon gas

C_D - Coefficient of drag

CH_{fa} - Convective heat transfer coefficient between the balloon film and air

CH_{gf} - Convective heat transfer coefficient between the balloon film and gas

D - Drag

$\dot{E}_g$ - Balloon gas volume flow rate for expelling gas when the maximum balloon volume is exceeded

$\dot{E}_v$ - Balloon gas mass flow rate during controlled valving operations

g - Acceleration due to gravity

G - Solar constant

Gr - Grashof number

k - Thermal conductivity

L - Characteristic length = 4/3 $\overline{R}$ for spheres

m_f - Mass of balloon film

m_g - Mass of balloon gas

m_{total} - Total mass of balloon system

M_a - Molecular weight of air

M_g - Molecular weight of the balloon gas

M_{H_2O} - Mass of trapped water vapor

Nu - Nusselt number

p_{a_1} - Ambient air pressure at the base of a layer in an atmosphere model

NOMENCLATURE (continued)

p_g - Pressure of the balloon gas

p_{H_2O} - Water partial pressure

Pr_a - Prandtl number of air

$\dot{q}_f$ - Net heat flux to balloon film

$\dot{q}_g$ - Net heat flux to the balloon gas

r_w - Reflectivity of the balloon film in the infrared spectrum

r_e - Earth reflectivity (albedo)

$r_{w,sol}$ - Reflectivity of the balloon film to solar radiation

R - Universal gas constant

$\overline{R}$ - Radius of an equivalent volume sphere

R_{ey} - Reynold's number

S - Balloon surface area = $4.835976\ V_g^{2/3}$

t - Time

T_a - Ambient air temperature

Ta_1 - Ambient air temperature at the base of a layer in an atmosphere model

T_{BB} - Black ball temperature

T_f - Balloon film temperature

T_g - Balloon gas temperature

V - Balloon volume

z - Balloon altitude

α_g - Absorptivity of the balloon gas to solar radiation

α_{geff} - Effective solar absorptivity of the balloon gas

α_w - Absorptivity of the balloon film in the infrared spectrum

$\alpha_{w,eff}$ - Effective solar absorptivity of the balloon film

NOMENCLATURE (continued)

$\alpha_{w,sol}$ - Absorptivity of the balloon film in the solar spectrum

ε_g - Emissivity of the balloon gas in the infrared spectrum

$\varepsilon_{g_{eff}}$ - Effective infrared emissivity of the balloon gas

ε_{int} - Effective interchange infrared emissivity

ε_w - Emissivity of the balloon film in the infrared spectrum

$\varepsilon_{w_{eff}}$ - Effective infrared emissivity of the balloon film

μ_a - Viscosity of the ambient air

ρ_a - Air density

ρ_{H_2O} - Water density

σ - Stefan-Boltzman constant

τ_w - Transmissivity of the balloon film in the infrared spectrum

$\tau_{w,sol}$ - Transmissivity of the balloon film to solar radiation

I. INTRODUCTION

For the past several years, the balloon user community has expressed considerable interest in the development of more reliable, heavier payload, and longer duration high altitude balloon systems. However, the successful design and operation of such systems requires an accurate knowledge and understanding not only of balloon gas and wall thermal variations but also of trajectory behavior. For example, the balloon lifting gas temperature is the primary factor controlling the balloon trajectory, the balloon lift, and the amount of lifting gas at float conditions. In turn, the coupling between ascent/descent rates and gas temperature strongly affects the balloon film temperature and, hence, its material properties. If the ascent velocity is too high, the film may cool below the cold-brittle point (about -80° for polyethylene) and experience catastrophic behavior. On the other hand, if the balloon expels too much gas during the daytime due to high gas temperatures or ballasting, it may experience an uncontrollable descent at sunset due to gas cooling. Obviously, an accurate understanding of these phenomena and a means of predicting them is essential for optimum flight control.

Consequently, during the past eighteen months, researchers at Texas A&M University (TAMU) have been engaged in the development of an up-to-date analytical and computer model suitable for obtaining engineering predictions of the trajectory and thermal performance of high altitude balloons. This report will review these efforts, present a new thermal and trajectory model, discuss typical results, and indicate those areas requiring further investigation. The associated computer program and instructions for its use are contained in Reference (1).

II. PREVIOUS STUDIES

Probably the first studies of balloon thermal behavior and its effect on flight performance were conducted by the University of Minnesota as part of the High Altitude Balloon Project in the 1950's. The results of this effort were primarily empirical and mainly concerned descent rates at sunset. In fact, after examining the governing equations, the study stated:[2]

> "Neither the functional form nor the values of the parameters are known well enough to make... ...reliable predictions of the behavior of an actual balloon."

This statement, however, did not deter investigators; and in 1966 Germeles[3] presented the first computer model based upon solution of the governing differential equations. Unfortunately, his predictions frequently did not agree with flight data; and his model contained significant errors in its formulation.[4]

Subsequently, several investigators[5-6] developed prediction methods based upon flight data and empirical curve fits. While these techniques are useful for performance estimates, they are frequently in error and are not based upon the fundamental physical phenomena governing the problem.

Now by far the most significant work to date associated with the prediction of the performance of high altitude balloons is that of Kreith and Kreider.[4,7] In a series of outstanding papers, they thoroughly discussed all pertinent phenomena, summarized existing knowledge, and developed an excellent model and computer program. Without a doubt, Ref. 4 was a benchmark effort; and thus, it has served as a starting point for all subsequent investigations.

In their model, Kreith and Kreider included the effects of direct and reflected solar radiation, earth and atmospheric infrared radiation, convection and radiative emission. They also considered adiabatic heating and cooling, gas expulsion, valving, ballasting, and sunrise and sunset. In many cases, the resultant predictions agreed well with flight data.

In addition, based upon the radiative properties of helium, the Kreith-Kreider model assumed that the lifting gas was completely transparent to all radiation. Consequently, under float conditions, the only mechanism heating or cooling the gas is convection between the gas and the film, which is proportional to the temperature difference $(T_f - T_g)$. Thus, the equilibrium gas temperature is equal to that of the film.

Simultaneously with these analytical developments, several investigations were conducted to measure lifting gas and balloon film temperatures in flight. The first of these were a series of flights by Lucas and Hall [8-10] using $7080m^3$ balloons which floated at 24 to 26 km and measured film and gas temperatures during ascent, float, and through sunrise and sunset. Subsequently, in 1975 and 1976, the National Scientific Balloon Facility (NSBF) conducted a series of engineering test flights carefully designed to measure gas and film temperatures on larger balloons at higher altitudes. The equilibrium float temperatures measured on these flights are shown on Table I, and the results were quite surprising.

Specifically, while the night values supported the thermal model assumption that equilibrium wall and gas temperatures should be the same, the daytime measurements consistently showed a significant difference with the lifting gas being warmer. In addition, since this phenomena only existed during daylight and, based upon the results of the RAD II and RAD III flights, was sensitive to the amount of albedo radiation, it appeared that the

FLIGHT		DAY			NIGHT		
		Altitude (km)	Gas (°C)	Film (°C)	Altitude (km)	Gas (°C)	Film (°C)
Boom V and Boom VII	Superpressure Mylar	29.3	-30	-40	29.3	-59	-59
RAD I	Zero Pressure Polyethylene 56634 m^3	33.5	-16.8	--	33.5	-47.4	--
RAD III	Zero Pressure Polyethylene 14160 m^3	29.7	-22	-37.5	29.0	-47	-47
Lucas-Hall	Zero Pressure Polyethylene 7080 m^3	24.4	-32	-39			
RAD II*	Zero Pressure Polyethylene 14160 m^3	29.7	-10	-36.5	25.9	-71	-71

Table I - Equilibrium Float Temperatures From Flight Measurements

* Overcast Skies; all other clear skies.

gas temperature enhancement was primarily due to solar radiation.

However, since helium is undoubtedly transparent to solar radiation at the temperatures present in a balloon gas, this phenomena is difficult to explain. One possibility is that during daylight, due to uneven heating the balloon film develops hot spots which through convection leads to a gas convection cell and a lifting gas supertemperature. Unfortunately, careful examination of the flight data did not reveal any film temperatures near or above the measured gas values; and thus, this explanation does not seem likely. In addition, predictions obtained with the Kreith-Kreider computer code consistently predicted float temperatures about 30°C below the measured gas values and about 5°C below the measured film values, indicating that in reality the gas was actually warming the film. Obviously, the gas was somehow being heated by solar radiation; and the existing transparent gas thermal models were inadequate.

Consequently, Carlson[11] developed a new thermal model, based upon engineering radiation concepts, which permitted the lifting gas to emit and absorb radiation in both the solar and IR spectra. Unfortunately, due to the lack of accurate film radiative property data, he was forced to simplify the model, to limit it to float conditions only, and to estimate film properties from flight data. Results obtained with this simplified model yielded excellent daytime values but consistently predicted night temperatures below those actually encountered in flight. Nevertheless, Carlson did develop a new complete thermal model compatible with flight experience which could be incorporated into a time dependent thermal and trajectory analysis method.

At about the same time, as part of the Heavy Load Balloon failure investigation[12], interest was revived in predicting the trajectory performance of high altitude balloons. Initial attempts using the Kreith-Kreider code

yielded discouraging results. Typically, when compared to actual flights, they predicted higher ascent rates below the tropopause and slower velocities above it. In addition, from flight thermal data it was known that Kreith-Kreider theoretically predicted incorrect float temperatures; and, in practice, it was cumbersome to use and difficult to modify.

Consequently, it was decided to develop a new trajectory and thermal analysis code incorporating the thermal model of Carlson which would, from an engineering standpoint, be sufficiently accurate for flight prediction or analysis. In addition, it was decided to make the code user oriented and structured in a manner which would easily permit changes as new knowledge became available. Finally, it was decided to limit this initial code to zero pressure ballons.

The remainder of this report will discuss this new model in detail and present results obtained with it.

III. THERMAL AND TRAJECTORY MODEL

A. Governing Equations

If it is assumed that the balloon trajectory problem can be treated two-dimensionally, (i.e. independent variables altitude, z, and time, t), and that the film temperature, T_f, and gas temperature, T_g, are spatially averaged values, then the governing differential equations are as follows:

Vertical Force Balance on the Balloon--

$$(m_{total} + 1/2\rho_a V)\frac{d^2z}{dt^2} = g(\rho_a V - m_{total}) - 1/2\rho_a C_D \frac{dz}{dt}\left|\frac{dz}{dt}\right| A \qquad (1)$$

(mass + virtual mass) acceleration = Lift - Drag

Heat Balance for the Balloon Film -

$$m_f c_f \frac{dT_f}{dt} = \dot{q}_f \qquad (2)$$

Heat Balance for the Lifting Gas -

$$m_g c_{pg} \frac{dT_g}{dt} = \dot{q}_g - \frac{M_a m_g T_g}{T_a M_g}\frac{dz}{dt} \qquad (3)$$

Mass Balance for the Lifting Gas -

$$\frac{dm_g}{dt} = \frac{p_g M_g}{R T_g} \dot{E}_g - \dot{E}_v \tag{4}$$

Where

$$\text{Volume} = V = \frac{m_g R T_g}{p_a M_g} \tag{5}$$

$$\text{Total Mass} = m_{total} = m_g + m_f + m_p \tag{6}$$

$$\text{Cross Sectional Area} = A = \pi \bar{R}^2 \tag{7}$$

$$\text{Surface Area} = S = 4\pi\bar{R}^2 \tag{8}$$

$\bar{R}$ = Radius of Equivalent Volume Sphere

It should be noted that Eqs. (1-8) are equivalent to those used by previous investigators[4], although the form of Eq. (3) is different due to the use of the specific heat, C_{pg}, instead of C_{vg}.

The forms for $\dot{q}_f$ and $\dot{q}_g$ are, however, different due to the incorporation of the new thermal model which permits gas emission and absorption. Following logic similar to that used in Ref. (11) and the engineering approach, as opposed to spectral, for radiative heat transfer[13], $\dot{q}_f$ and $\dot{q}_g$ can be expressed as

$$\dot{q}_f = [G\alpha_{weff}(1/4+1/2r_e) + \epsilon_{int}\sigma (T_g^4 - T_f^4)$$

Net flux to film: solar + Albedo; IR interchange between gas and film

$$+ CH_{gf}(T_g - T_f) + CH_{fa}(T_a - T_f)$$

convection between gas & film; convection between air & film

$$-\epsilon_{weff}\sigma T_f^4 + \epsilon_{weff}\sigma T_{BB}^4] S \tag{9}$$

film IR emission; earth-air IR input

and

$$\dot{q}_g = [G\alpha_{geff}(1 + r_e) - \varepsilon_{int}\,\sigma(T_g^4 - T_f^4)$$

Solar + Albedo; IR interchange between gas and film

$$-CH_{gf}(T_g - T_f) - \varepsilon_{geff}\,\sigma T_g^4$$

convection between gas and film; Gas IR emission

$$+\varepsilon_{geff}\,\sigma T_{BB}^4\,]\,S \qquad (10)$$

Earth-air IR input

Since balloon film is semi-transparent, any radiation to or from the balloon film will be partially transmitted, and then partially transmitted off the opposite wall an infinite number of times. Thus, in Eqs.(9) and (10) α_{weff} ε_{int}, ε_{weff}, α_{geff}, and ε_{geff} are effective coeffieients which take into account this multiple pass phenomena. Based upon Ref. (11), these quantities are defined in terms of the actual gas and wall radiative properties as

$$\alpha_{weff} = \alpha_w\left[1 + \frac{\tau_{w,sol}\,(1-\alpha_g)}{(1 - r_{w,sol}(1-\alpha_g))}\right] \qquad (11)$$

$$\varepsilon_{int} = \frac{\varepsilon_g\,\varepsilon_w}{1-r_w(1-\varepsilon_g)} \qquad (12)$$

$$\varepsilon_{w,eff} = \varepsilon_w\left[1 + \frac{\tau_w(1-\varepsilon_g)}{(1-r_w)}(1-\varepsilon_g)\right] \qquad (13)$$

$$\alpha_{geff} = \frac{\alpha_g\,\tau_{w,sol}}{1-r_{wsol}(1-\alpha_g)} \qquad (14)$$

$$\varepsilon_{geff} = \frac{\varepsilon_g \tau_w}{1-r_w(1-\varepsilon_g)} \tag{15}$$

If it were assumed that the lifting gas is transparent and does not emit or absorb (i.e. $\alpha_g = \varepsilon_g = 0$), Eqs. (11-15) reduce to the multiple pass effective coefficients,

$$\alpha_{weff} = \alpha_w \left(1 + \frac{\tau_{wsol}}{1-r_{wsol}} \right) \tag{16}$$

$$\varepsilon_{weff} = \varepsilon_w \left(1 + \frac{\tau_w}{1-r_w} \right) \tag{17}$$

which correspond to those used in Ref. (4).

With proper input, initial values, and definitions, Eqs. (1-17) form a well posed initial value problem for z, $\frac{dz}{dt}$, T_f, T_g, m_g, and volume.

B. Gas Radiative Properties

Since the present model permits the gas to radiatively emit and absorb, estimates for α_g and ε_g must be made. At this point, it should be noted that in engineering the phrases absorption coefficient, absorptivity, and the symbol α refer to radiative properties associated with the solar spectrum; while, on the other hand, emission coefficient, emissivity, and ε refer to the infrared spectral region. This distinction of terms was adopted for this investigation also.

Now before α_g and ε_g can be estimated, an explanation for the lifting gas radiative behavior needs to be postulated. An examination of helium reveals that it does contain several spectral lines in the solar spectrum.[14] However, these transitions are all between excited states; and at the temperatures present in balloons, the number of atoms in these states would be negligible. Consequently, it is highly unlikely that helium would directly absorb solar energy.

Another possibility is that the lifting gas contains a small amount of some contaminant which is intensely absorbing in the solar spectrum. This absorption would increase the energy and hence the temperature of the contaminant, and it would subsequently be rapidly transferred to the helium via particle-particle collisions.

One possibility for this contaminant is water vapor, whose presence in even trace amounts is well known to drastically affect spectral measurements based on radiative processes. Interestingly, water vapor has in the solar spectrum intensely absorbing bands at [4,13] 0.75, 0.78, 0.85, 0.95, 1.15, 1.4, and 1.9 microns; and based on re-entry radiative gas dynamics, such bands can significantly affect the overall radiation properties of the gas, even if they are narrow.[15] Consequently, if water vapor is present in the lifting gas in a trace amount, it could be the origin of the observed gas temperature enhancement.

One possible source of water vapor in balloons is in the air trapped inside it during manufacturing and packaging. If it is assumed that a balloon is assembled at 80% relative humidity, and 25°C, and packed with a 0.15875 cm layer of air trapped inside, then the amount of water contained in the balloon would range from 200 gm for a small balloon to 2300 gm for a large one. At a float altitude of 32 km and a gas temperature of about -15°C, the partial pressure of this water would range from 2 to 4 dynes/cm^2. Since at these conditions, the maximum vapor pressure of water vapor over ice is about 1650 dynes/cm^2, all of the water would be in vapor form and available for radiative absorption.

At this point, it should be pointed out that this water vapor explanation may be totally incorrect; and its verification depends upon future research. Nevertheless, as subsequently shown in this section and in the discussion of

typical results later in this report, exact knowledge of the contaminant is not required.

Now fortunately, the radiative properties of water vapor in the infrared are well known and documented; [13] and in general, the emissivity of such vapor can be expressed as

$$\varepsilon_g = A(p_{H_2O}L)^B \tag{18}$$

where p_{H_2O} is the water partial pressure and L is a characteristic length equal to 4/3 R for spheres. If R is the float radius and t is the thickness of the trapped layer during packaging, then the mass of trapped water is

$$M_{H_2O} = \rho_{H_2O} \; 4\pi R^2 t \tag{19}$$

where $\rho_{H_2O_m}$ is the water density at manufacture. Then at float the vapor partial pressure is

$$p_{H_2O} = 3\rho_{H_2O} \; \frac{t}{R} \; \frac{RT_g}{M_{H_2O}} \tag{20}$$

and

$$p_{h2o} \; L = 4 \; \rho_{H_2O_m} \; t \; \frac{RT_g}{M_{H_2O}} \tag{21}$$

For 80% relative humidity, 25°C, and 0.15875 cm initial conditions, this equation simply becomes

$$p_{H_2O} \; L = 1.746 \times 10^{-6} \; T_g \tag{22}$$

where $p_{H_2O} \; L$ is in ft-atm and T_g is in °K. A correlation of the data in Ref. (13) at conditions covering those encountered by a high altitude balloon yields

$$\varepsilon_g = 0.16907 \; (p_{H_2O} \; L)^{.8152} \tag{23}$$

Thus, by combining Eqs. (22) and (23), an equation suitable for estimating the gas emissivity can be found, i.e.

$$\varepsilon_g = 0.169\ (1.746 \times 10^{-6}\ T_g)^{.8152} \qquad (24)$$

where T_g is in °K.

Based upon experimental data, float gas temperatures can range from 233°K to 273°K, which yields ε_g values from 0.00029 to 0.00033. These values of emissivity are very small, and their effect on balloon thermal behavior will be almost negligible. Furthermore, since the range of ε_g is very small over the entire range of balloon float gas temperatures, the value for T_g need only be approximated Eq.(24) in order to obtain an accurate estimate of ε_g.

Unfortunately, the absorptivity radiative properties of water are not documented in engineering form since radiative properties of water are not encountered in normal heat transfer problems. However, α_g can be estimated by using the equilibrium float program, THERMNEW,[11,16] and finding the absorptivity necessary to reproduce experimental flight gas temperatures. This procedure was applied to a variety of balloons and the required α_g was consistently found to be in the range

$$0.0026 \leq \alpha_g \leq 0.0030 \qquad (25)$$

Note that since this procedure is based upon experimental data, the resultant α_g values are independent of the actual contaminant.

Now the results expressed in Eq. (25) have several interesting features. First, the value of α_g is essentially constant and apparently only a weak function of gas temperature and size, which is in agreement with the trend given for emissivity by Eq. (24). Second, the required values for α_g are an order of magnitude larger than those for ε_g. However, experience[15] with re-entry radiative transfer indicates that spectral regions dominated by line absorption frequently have absorption coefficients orders of magnitude larger than other regions. Thus, this result appears logical.

Based upon the approach used for emissivity, α_g might have a functional form of

$$\alpha_g = C[T_g^{1/3} p_a^{2/3}]^B \quad (26)$$

Correlations with this form were tried in several tests, but in general the thermal results differed from those using a constant α_g by only about 1°K. Consequently, based upon these studies and the small variation expressed in Eq. (25), it is believed that good results can be obtained using a constant value for α_g.

C. Film Radiative Properties

As shown by many investigations,[4,11] one of the primary factors affecting balloon trajectory and thermal performance is the radiative properties of the balloon film, i.e. absorptivity/emissivity, transmissivity, and reflectivity in both the IR and solar. Unfortunately, previous estimates[11] of these quantities have varied so widely that their application to performance analyses has been essentially worthless. Since 1975, however, several attempts[17-19] have been made to accurately measure these properties in the laboratory; and some typical results are shown on Table II.

Examination of these data indicate that the LRC (1975) and LRC (1980) measurements are in relatively good agreement. However, the LRC and JSC(1975) results disagree significantly, particularly with respect to $\alpha_{w,sol}$ and ε_w. Subsequent discussion with the manufacturer of the equipment used in the tests indicates that JSC probably used an incorrect value for the equipment backing reflectivity used in reducing the data and incorrectly matched wavelengths. Consequently, the JSC measurements were re-reduced using correct backing values and wavelength regions; and the results are shown on Table II as JSC (Mod). As can be seen, these modified values agree quite well in the solar

MATERIAL	SOURCE	SOLAR			IR		
		$\tau_{w,sol}$	$r_{w,sol}$	$\alpha_{w,sol}$	τ_w	r_w	ε_w
Stratofilm ½ mil	JSC(1975)	.87	.090	.040	.854	.071	.075
	JSC(Mod)	.88	.120	.000			
	LRC(1980)	.886	.112	.0016	..852	.131	.0171
Polyethylene 6 mil	LRC(1975)	.89	.10	.01	.86	.10	.04
Stratofilm 1 mil	JSC(1975)	.87	.084	.046	.831	.068	.101
	JSC(Mod)	.88	.114	.006	.831	.024	.145
	LRC(1980)	.885	.114	.001	.842	.127	.031

Table II - Measured Film Radiative Properties

region with the LRC (1980) results. Since these data sets were obtained with different techniques and equipment, it is believed that the resultant LRC (1980) solar values are excellent and as good as can be obtained with present equipment and techniques.

In the IR spectra, unfortunately, the JSC (Mod) and LRC (1980) still disagree with respect to measured reflectivity. (The emissivity, ε, is not directly measured but deduced from measurements of τ and R.) Examination of the JSC test and instrument calibration data on opaque samples provided with the film results has revealed, however, that the JSC IR reflectivity are always way below accepted values. Thus, it is believed that the JSC emissivity and reflectivity values in the infrared are in error.

Consequently, in the present investigation, the following values have been used for the radiative properties of balloon film:

$$\alpha_{w,sol} = 0.001 \quad r_{w,sol} = 0.114 \quad \tau_{w,sol} = 0.885$$

$$\varepsilon_w = 0.031 \quad r_w = 0.127 \quad \tau_w = 0.842$$

As will be seen, the usage of these values consistently leads to excellent temperature predictions.

Finally, based upon these measurements, it should be noted that the solar absorptivity of balloon film is extremely small. As a consequence, solar heating, either directly or via the albedo effect, will only slightly affect the film temperature; and, thus, it is unlikely that the daytime gas superheat is due to uneven solar heating of the balloon film. In other words, since the day-night IR heating is the same, these measurements verify that the daytime temperature enhancement of both the gas and the skin must be due to solar absorption in the lifting gas and subsequent heat transfer to the balloon film.

D. Balloon Drag Coefficient

As can be seen in Eq. (1), one of the primary forces acting on a balloon is drag; and to predict this force correctly, an accurate knowledge of the appropriate drag coefficient variation is required. Unfortunately, most wind tunnel tests on balloon shapes, such as Ref. (20) are for tethered balloons in which the free stream is horizontal and not vertical as in the present problem. Consequently, previous investigators[4,5] have resorted to using an equivalent sphere model for which

$$\text{Drag} = D = 1/2\rho \left|\frac{dz}{dz}\right| \frac{dz}{dz} \quad C_D \quad A \tag{27}$$

where A is cross-sectional area of an equivalent volume sphere, i.e.

$$A = \pi \bar{R}^2 \tag{28}$$

and C_D is the drag coefficient for a sphere. Since sphere data is available and since over much of the flight profile the balloon shape is close to a sphere, this approach is also used in the present investigation.

Unfortunately, there exists disagreement in the literature as to the appropriate sphere values to use for balloons. Figure 1 plots various correlations for C_D over the Reynolds number range normally encountered during ascent. Here

$$\text{Reynolds No.} = \text{Rey} = \frac{\rho_a \left|\frac{dz}{dt}\right| (2\bar{R})}{\mu_a} \tag{29}$$

The curve designated Kreith[4] is an accurate straight line approximation to accepted smooth sphere values,[21] and it was used in the original version of Reference 4. However, application of this correlation consistently led to high predictions for ascent rates below the tropopause in typical balloon flights. In this portion of the flight, a balloon typically encounters Reynolds numbers between 3×10^5 and 3×10^6. Consequently, in the revised version of Ref. 4, Kreith and Kreider arbitrarily increased

C_D to a value of 0.5 for all Reynolds numbers above 3×10^5. This action did significantly improve the accuracy of their method below the tropopause.

In a different approach, Nelson[4] rationalized that during ascent a balloon is essentially a sphere-cone shape and should have a drag coefficient lower than that of a sphere. Consequently, he used 54% of the sphere values given in Ref. 2 during ascent and the full value during descent. This 54% curve is shown in Fig. 1 as Winzen.

As part of the present investigation, the effect of C_D on balloon ascent behavior was carefully studied; and it was determined that balloon ascent velocities between launch and the tropopause are very sensitive to the values of C_D. In fact, the present results agree with those of Kreith and Kreider in that the usual sphere value of about 0.1 is too low and that a value around 0.5 is more reasonable.

One possible explanation for this larger drag coefficient is that the balloon is a large system with extensive surface area, and thus it would experience significant skin friction drag in addition to the pressure drag normally found on a sphere. Studies of this possibility indicate that, including skin friction effects, a value of 0.35 could be possible. Nevertheless, even with this explanation, the C_D should experience a decrease between 10^5 and 3×10^5 due to transition from laminar flow to turbulent flow. This "transition" phenomena moves the boundary layer separation point rearward and results in a significant decrease in initial drag.

Another possibility is that during ascent, the balloon apex region is more oblate than a sphere due to pressure differences across the film.

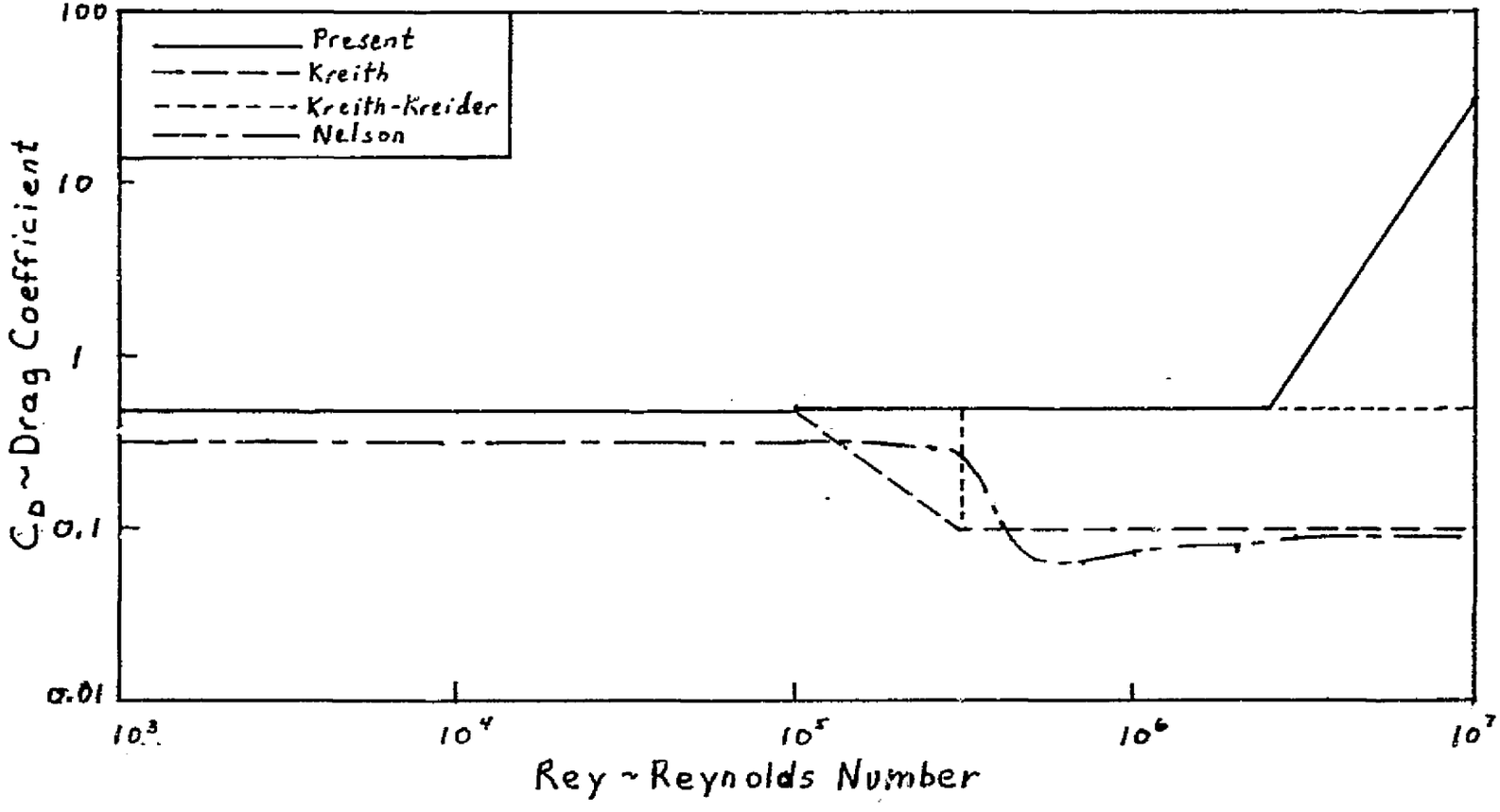

Figure 1 ~ Drag Correlations

Such a shape change would increase the effective drag coefficient, but a laminar-turbulent break would still be expected.

Now from an aerodynamicist's point-of-view, the present required C_D variation with Reynolds number has the appearance of a flow characterized by a laminar rather than a turbulent separation. In 1935, Hoerner[23] performed drag measurements on smooth and rough spheres; and he found that on rough spheres the drag coefficient never had the laminar turbulent decrease typical of smooth spheres. In fact, he determined that C_D remained essentially constant at about 0.47 to 0.5 well up into the 10^6 Reynolds number range. He postulated that the boundary layer was separating laminarly and never reattaching. Today, it is known[24] from detailed tests and numerical studies, that on blunt nosed airfoils the flow usually separates laminarly near the leading edge, transitions to turbulent flow above the resultant small separation bubble, reattaches, and then turbulently separates far downstream near the trailing edge. However, under certain low local Reynolds numbers conditions, the flow separates laminarly, transitions, but never reattaches. Thus, Hoerner's explanation seems to be in agreement with both balloon and airfoil data; and thus the existence of an essentially constant drag coefficient over much of the flight regime of a balloon appears reasonable. Apparently, a balloon behaves similarly to that of a rough sphere in a wind tunnel.

Unfortunately, there exists almost no experimental wind tunnel drag data for spheres at Reynolds numbers above 1×10^6. However, modern heavy lift balloons, which have float volumes greater than $5 \times 10^5 m^3$, have ascent Reynolds numbers significantly above 2.5×10^6 in the region between launch and the tropopause. Initial attempts to model such flights were unsuccessful in that they predicted excessive ascent velocities below the

tropopause. Since these flights represented the only experimental data available for large spheres at large Reynolds numbers, these data[25] were used to estimate appropriate drag coefficients for Rey > 2.5×10^6. Subsequent correlation yielded the curve shown on Fig. 1.

At first, the sharp increase in drag coefficient above 2.5×10^6 might seem unreasonable. However, during the early stages of ascent the shape of a large volume balloon is significantly different from that of a sphere. Thus, the present large C_D values probably simply reflect the usage of an equivalent sphere cross-sectional reference area in the formulation of drag.

In conclusion, based upon the present research and an analysis of previous studies and efforts, the following are believed to be suitable estimates of the drag coefficient of a balloon, as defined by Eqs. (27-29):

$$
\begin{aligned}
&\text{Rey} < 10^{-2} && C_D = 2400 \\
&10^{-2} < \text{Rey} < 10^{0} && C_D = 24/\text{Rey} \\
&10^{0} < \text{Rey} < 10^{1} && C_D = 24\ \text{Rey}^{-0.757} \\
&10^{1} < \text{Rey} < 10^{2} && C_D = 16.04\ \text{Rey}^{-0.582} \\
&10^{2} < \text{Rey} < 10^{3} && C_D = 6.025\ \text{Rey}^{-0.369} \\
&10^{3} < \text{Rey} < 10^{5} && C_D = 0.47 \\
&10^{5} < \text{Rey} < 2.5 \times 10^{6} && C_D = 0.5 \\
&2.5 \times 10^{6} < \text{Rey} && C_D = 6.7297 \times 10^{-20}\ \text{Rey}^{2.9495}
\end{aligned}
\qquad (30)
$$

Equations (30) are used whenever dz/dt is positive. When dz/dt is negative, these values are arbitrarily doubled.

E. Heat Transfer Coefficients

In the present model, one of the important factors affecting the gas and film temperatures is the heat transfer between the film and the ambient

atmosphere and the lifting gas. Historically, this heat transfer is usually expressed in terms of a heat transfer coefficient, which in turn is correlated as a Nusselt number, i.e.

$$q = CH\ (\Delta T)\ A$$

$$Nu = \frac{(CH)\ L}{k} \tag{30}$$

Here L is a characteristic length and k is the thermal conductivity of the adjacent gas.

For a balloon, the heat transfer between the film and the air can be either forced, which depends upon the velocity and character of the surrounding flowfield and occurs during ascent or descent, or natural, which occurs when the balloon is at rest or at very low velocity. While very little information exists for sphere or balloon like shapes in the regimes of interest for balloon flight, the present research indicates that the following are adequate:

Natural Convection--Film-Air

$$Nu = 2 + 0.6\ (GrPr_a)^{\frac{1}{4}} \tag{31}$$

Forced Convection--Film-Air

$$Nu = 0.37\ (Rey)^{0.6} \tag{32}$$

Here Gr is the Grashof number as usually defined, Pr_a is the Prandtl number of air (about 0.72), and Rey is the same as Eq. (29). Eq. (31) has the correct lower limit of two and is identical to that used by Kreith-Kreider.[4] Since it is only used at float conditions where convection is small compared to radiative effects, Eq. (31) should suffice.

Forced convection, however, is important in that it significantly affects the balloon film temperature during ascent. Eq. (32) is the widely accepted form due to McAdams and reported by Kreith,[26] and it's based upon experimental data at $10 < Rey < 10^5$. It yields greater values for Nu than the basic form given by Ref. (4) of

$$Nu = 2 + 0.419\ (Rey)^{0.55} \tag{33}$$

However, Ref. (4) suggests multiplying Eq. (33) by at least a factor of 1.5 in order to obtain results in agreement with balloon flight data. This multiplication results in Nusselt number values very close to those given by Eq. (32).

As previously indicated, Eq. (32) is based upon Rey less than 10^5, while modern balloons have Reynolds numbers during ascent in the range 10^5 to 10^7. For small balloons, the results of the present research indicate that Eq. (32) is adequate. However, for large systems (maximum volumes above $5.38 \times 10^5 m^3$), it appears to under predict the film-air heat transfer. Since balloon flight tests represent the only available data for large spheres, flight trajectory data have been used to deduce the applicable coefficient form. Thus, in the present model, for balloons having maximum volumes greater than $5.38 \times 10^5 m^3$, Eq. (32) is replaced by

$$Nu = 0.74\ (Rey)^{0.6} \tag{34}$$

This factor of two increase is strictly empirical and is strictly justified by the fact that its application yields predictions in agreement with flight test data. In addition, it should be noted that attempts to combine Eqs. (32) and (34) into a unified formula were unsuccessful. Obviously, it is an area which requires further research.

Finally, with respect to film-air convection, the actual heat transfer should transition smoothly from forced to natural convection as the balloon goes into float. Since the balloon enters float in an oscillatory manner, the exact method of modeling this transition is unclear. In the present research, it has been found adequate to use the larger of the values predicted by Eq. (31) and (32).

For convection inside the balloon, Kreith[27] suggests usage of the following:

$$\begin{aligned} Nu &= .59\ (GrPr_g)^{1/4}, \quad (Gr.Pr_g) < 10^9 \\ &= .13(GrPr_g)^{1/3}, \quad (Gr.Pr_g) > 10^9 \end{aligned} \tag{35}$$

Where Pr_g is the Prandtl number of the lifting gas (about 0.67 for Helium). The break corresponds to the transition from laminar to turbulent flow in the convection induced flow inside the balloon. In Ref. (4), Kreith and Kreider found that the usage of these formulas resulted in a delay in gas heating above the troposphere and subsequently in excessively low ascent velocities. Thus, they arbitrarily used a factor of three on Eq. (35).

A need for similar enhancement has been found in the present research, although a factor of 2.5 has been found to yield the best correlation. Thus, in the present model, the following gas-film Nusselt number correlations have been used:

$$\begin{aligned} Nu &= 2.5(2 + 0.6\ (Gr{\cdot}Pr_g)^{1/4}), \quad Gr.Pr < 1.5 \times 10^8 \\ &\quad 0.325(Gr.Pr_g)^{1/3}, \quad Gr{\cdot}Pr_g > 1.5 \times 10^8 \end{aligned} \tag{36}$$

In Eqs. (36), the breakpoint has been chosen so as to yield a smooth transition between the two formulas.

Now, Eqs. (35) are based upon experiments conducted on one inch spheres with sub-cooled nitrogen. Thus, they are probably not directly applicable to balloons; and the necessity for modification should not be surprising.

F. Atmospheric Model

In any model for balloon performance, the variation in atmospheric properties with altitude must be represented accurately since these properties directly affect balloon lift, drag, and heat transfer. Fortunately, the variation in ambient temperature with altitude is well behaved in that the lapse rate, dT/dz, is essentially constant over well defined layers. As a result, by specifying the temperature at specific altitudes and assuming a constant lapse rate in between, the pressure at any altitude within a layer can be computed from

$$p_a = p_{a_1} / \left(\frac{Ta}{Ta_1}\right)^{\frac{gM_a}{RdT/dz}} \tag{37}$$

where P_{a_1}, and T_{a_1} are the condition at the bottom of the layer. The ambient density can then be evaluated via

$$\rho_a = \frac{p_a M_a}{RT_a} \tag{38}$$

Obviously, as many layers as desired can be used; but a large number of layers will result in excessive computer time.

Consequently, in an attempt to keep the present method as simple as possible, only two layers were initially used. This approach

specified the launch temperature and pressure, temperature at the tropopause, and temperature at float. However, examination of altitude temperature profiles at Palestine, Texas and the 1962 Standard Atmosphere,[20] revealed that such an approximation was too simple and did not adequately model the atmosphere in the vicinity of the tropopause or at altitudes above 32 km.

Consequently, a four segment temperature profile model has been developed and incorporated into the numerical method. This approach accurately models the 1962 Standard Atmosphere and adequately represents the seasonal profiles encountered at the major launch site at Palestine, Texas. These profiles are shown on Figure 2; and, as can be seen, the standard atmosphere is a poor representation much of the year. In the actual program,[1] these profiles can be easily selected via a single parameter input; or the user can utilize his own four segment profile.

Limited studies with these profiles reveal that ascent trajectories and float pressure altitude are only slightly affected by profile choice. However, float altitude may vary as much as 500 meters.

Finally, in the atmospheric model, air thermal conductivity is assumed constant; and air viscosity is computed via a cubic curve fit versus altitude. It is believed that these representations are adequate for balloon flights.

G. Blackball Model

To date the most accurate and convenient method of representing the earth-air infrared radiative input to a balloon is via the blackball concept,[4] and this approach had been used in Eqs. (9) and (10). Its application, however, requires an accurate representation

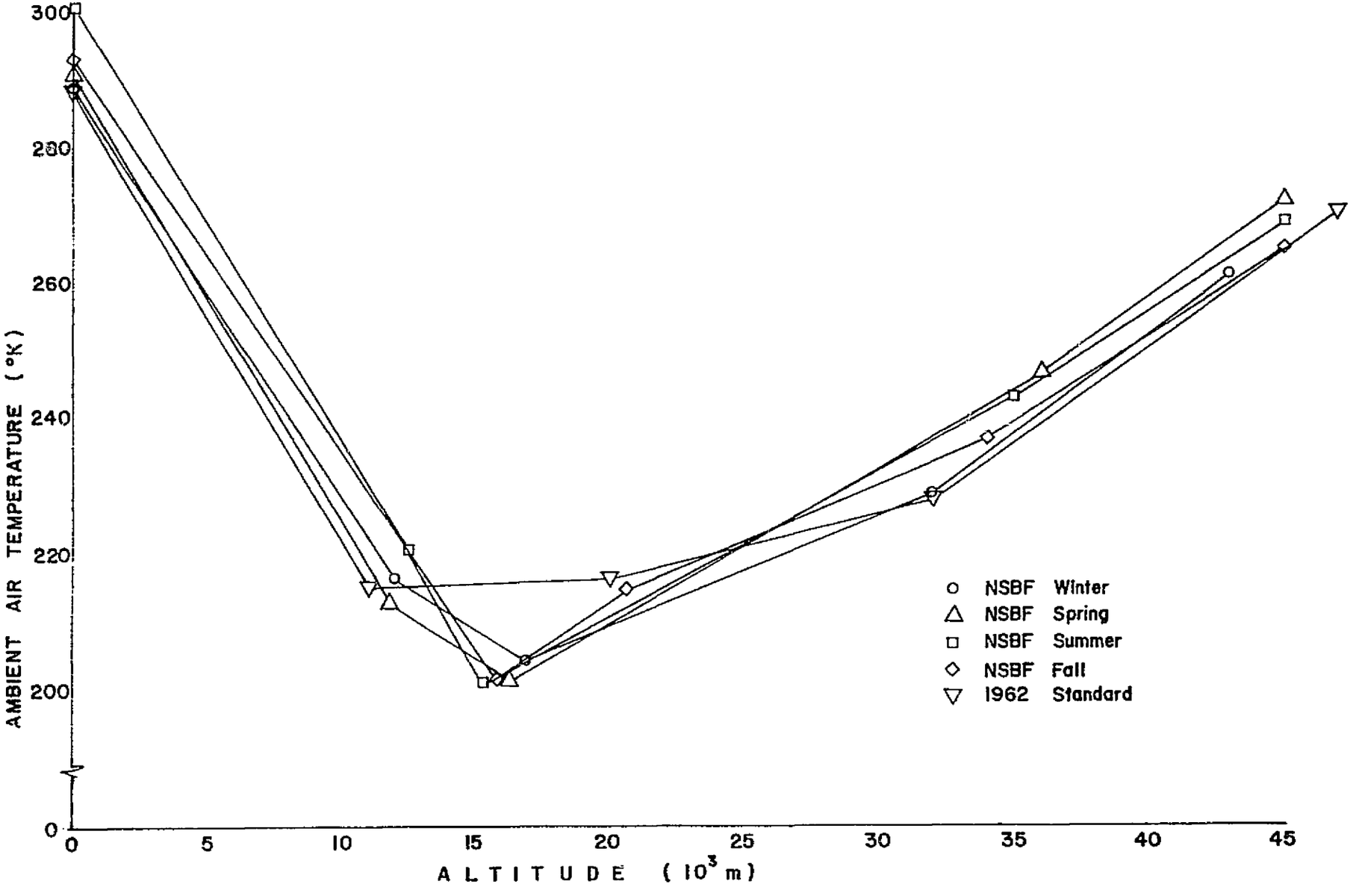

Figure 2. Five optional atmospheric temperature profiles available in the THERMTRAJ program

of the blackball temperature versus altitude. Normally, T_{BB} decreases linearly from a launch value slightly below ambient to a value at the tropopause. Above the tropopause, T_{BB} is normally constant, since most of the radiative input is from below.

The tropopause value, however, is strongly dependent upon cloud cover since clouds, due to their water content, absorb much of the radiation in the infrared. Consequently, in the present model, the following values are normally used:

Clear Skies--

At launch $$T_{BB} = T_{a_{launch}} - 5.5^{\circ}K$$

(39)

At tropopause and above

$$T_{BB} = 214.4^{\circ}K$$

Overcast Skies--

At launch $$T_{BB} = T_{a_{launch}} - 5.5^{\circ}K$$

(40)

At tropopause and above

$$T_{BB} = 194.4^{\circ}K$$

The variation with partially cloudy conditions will be discussed in the next section.

Now unfortunately, conditions are occasionally such that significant variations occur from the standard profiles represented by Eqs. (39-40). Usually, such variations could be expected after

a long heat wave and/or dry spell, and such an occurrence did happen on the RAD III flight. In that case, the launch was at night and accurate blackball temperatures were measured throughout ascent. These temperatures could be accurately approximated by a linear variation between the following points:

Launch	$T_{BB} = 309.6^{\circ}K$	
16400m	$250^{\circ}K$	
24500m	$250^{\circ}K$	(41)
29100m	$225^{\circ}K$	
Above 29100m	$225^{\circ}K$	

An attempt to model this flight using the standard clear sky profile, Eq. (39), was in general unsatisfactory; and, thus, the numerical model has been modified to permit a four segment blackball profile. As will be shown in section V, usage of the Eq. (41) values in this four segment representation was very successful for the RAD III flight.

Nevertheless, these results indicate that ascent trajectories are sensitive to earth-infrared behavior and that significant anomolies from "standard profiles" can occur. This possibility and sensitivity, of course, poses difficulties to an individual trying to predict a flight in advance and must be suitably considered.

H. Cloud Simulation

From the earliest attempts to analyze high altitude balloon performance,[2] it has been recognized that the presence of clouds significantly affects balloon behavior. Basically, the presence of clouds below a balloon reflects sunlight back to the balloon, thus

increasing the solar input, and absorbs part of the earth-air infrared radiation. While clouds also radiate infrared energy, they do so at a characteristic temperature lower than that of the earth, and so the total effect of clouds is to reduce the infrared radiative input to the balloon system while increasing the solar input. The combined effects may lead to either a daytime heating or cooling of the balloon, depending upon the relative radiative properties of the balloon film and gas. At night, clouds always cause a temperature decrease due to the lowering of the infrared input.

As a result of their importance, many attempts have been made to correlate albedo, r_e, and blackball temperatures, T_{BB}, as a function of cloud cover and cloud type; and these efforts are thoroughly reviewed in Ref. (4) and (29). In summary, it is now generally accepted that the following values are appropriate for flights over land:

Clear Skies: $r_e = 0.18$, $T_{BB} = 214.4^{\circ}K$

Overcast Skies: $r_e = 0.57$, $T_{BB} = 194.4^{\circ}K$

In addition, based on the results presented in Ref. (4), it is appropriate to assume a linear variation with percent cloud cover for these quantities.

This approach has been used to study the effects of cloud cover on Flight 1131PT, which was launched at sunset and for which minimal cloud data was recorded. On this flight, the skies were clear for the first fifty minutes. Between 50 and 90 minutes after launch the sky was 100% overcast, while after 90 minutes the balloon was over a 50% overcast.

The simulation results for this flight predict a time to float of 197 minutes if the skies were clear, and 224 minutes for the observed conditions. Obviously, for a night ascent, the presence of clouds causes a cooling of the balloon and a lower ascent rate.

During the day, various investigators disagree as to the expected behavior. Reference (2) says that a balloon floating over high clouds will descend even during the day, while the results presented in Ref. (29) indicate that the balloon film and gas will increase in temperature and will rise and/or expel gas. The latter is in pseudo-agreement with the observed behavior of RAD II.

An analysis of these studies indicates that the type of clouds strongly influences the resultant behavior. A thick, low overcast will have a high albedo which may overcome the decrease in IR radiation and lead to increased balloon temperature. High clouds, such as thin cirrus, which may not even be visible from the ground have, however, a low albedo. They may, thus, only serve to decrease the infrared input to the balloon and lead to a decrease in temperatures and subsequent descent.

Hauchecorne and Pomnerau[30] have extensively investigated cloud effects experimentally, and they report significant differences for the two cases. For a low overcast composed of cumulus-nimbus clouds, they found a high albedo reflectivity of 0.58. However, for high thin cirrus, their measurements indicate characteristic blackball temperatures of 202 to 208°K and an albedo of only 0.20. The latter is only slightly above the clear earth value of 0.18 to 0.19.

In addition, as part of the present research, Flight 167N, which encountered high cirrus during daytime float, has been modeled; and it has been determined that such clouds have an effective albedo of about 0.18 and a blackball temperature of 204.4°K.

Based upon these studies, the following correlations and values are recommended for use in the present model.

$$\text{Albedo:} \quad r_e = 0.18 + 0.39 \text{ (\% cloud cover)} \tag{43}$$

Since the solar absorptivity of polyethylene balloon film is extremely low, the albedo effect will be minimal; and Eq. (43) probably can be used for all types of clouds. However, for thin cirrus, an r_e of 0.18 is still suggested.

Blackball Temperature:

For low altitude and or thick clouds

$$T_{BB} = 214.4 - 20 \text{ (\% cloud cover)} \tag{44}$$

For thin high cirrus

$$T_{BB} = 204.4^{\circ}K \tag{45}$$

In the actual computer program,[1] albedo values are controlled via an input array versus time from launch. The actual values can be determined via Eq. (43). For blackball temperatures, the values during ascent are controlled via the four segment profile discussed previously. After arrival at float, they are determined via an input array versus time from launch. Again, the actual input values must be determined by the user from Eqs. (44-45).

I. Gas Expulsion, Valving and Ballasting

Due to environmental conditions and operational requirements, a balloon may undergo gas expulsion, valving, and/or ballasting

during the course of its flight. Gas expulsion, sometimes called burping, occurs whenever the balloon is at its maximum volume and continues to ascend due to inertia and momentum. Since a zero pressure balloon is always launched with excess free lift and hence gas, this phenomena almost always occurs as the balloon goes into float. It can also take place if the balloon is at its maximum volume and the gas is subsequently heated, say due to sunrise.

In the present model, gas expulsion is handled straightforwardly. If at the end of a computational time step the calculated volume exceeds the maximum possible, the time step is repeated with a volumetric expulsion rate of

$$\dot{E}_g = - \frac{V_{calculated} - V_{max}}{\Delta t} \tag{46}$$

This term is used in Eq. (4) where it is converted to a mass flow rate. If the new volume still exceeds V_{max}, $\dot{E}_g$ is doubled and the process repeated. This procedure is continued until a volume less than or equal to the maximum is acheived. In practice, this approach to burping has been found to be simple, reliable, and realistic.

Since in many flights operational specifications may require an increase or decrease in ascent or descent velocities, the model also permits arbitrary gas valving and ballasting. Approximately twelve valvings and 50 ballast drops of arbitrary length and mass rate (gm/min) can be treated with the present program configuration. These are handled via $\dot{E}_v$ in Eq. (4) and time variations in payload mass, m_p, in Eq. (6), respectively.

Tests with the method indicate that valving and ballasting must be accurately represented if a flight is to be correctly simulated.

IV. COMMENTS ON APPLICATION

While in general the model and associated computer program has and should be applied in the manner described in Ref. (1), several comments can be made concerning certain details. This section will discuss a few of these areas.

An item of importance in the application of any initial value thermal analysis is the appropriate thermal starting conditions at launch. The inflation process, however, is very complicated. First the gas undergoes a Joule-Thomson throttling process in exiting the high pressure gas bottles into the low pressure fill tube. Then, while traversing the fill tube to the balloon, the gas experiences a nonisentropic combination Rayleigh-Fanno flow involving complicated heat transfer and viscous friction phenomena. Finally, upon exiting the fill tube into the balloon, the gas is adiabatically expanded.

In the Joule-Thomson process, the gas behaves, due to the high initial pressure, imperfectly and as a result of a negative Joule-Thomson coefficient probably increases in temperature. In the adiabatic expansion, however, the gas is cooled to T, where

$$T = \frac{T_{inlet}}{c_p/c_v} \tag{47}$$

Thus, those two effects tend to counterbalance each other.

In addition, the inflation time of a typical balloon ranges from five to fifteen minutes. Based upon calculations performed early in the present research program, only a few minutes are

needed for the system to achieve thermal equilibrium at the launch ambient temperature. Also, sensitivity studies performed with the present model indicate that the effects of initial temperatures are rapidly "forgotton" and that overall results are not sensitive to the starting temperature values. Consequently, the model assumes that the initial values for the gas and film temperatures are the launch ambient air temperature.

Another item of importance in the solution of a set of differential equations is the method of solution. Such a method should be simple, straightforward, and easily understood by a potential user; and yet it should be accurate and stable. Consequently, the standard Runge-Kutta Method of order four has been used in the present program. This well known method works well for nonlinear initial value systems of ordinary differential equations and only has an error proportional to the time step to the fourth power.

Obviously, the successful application of such a method requires the usage of a sufficiently small time step. Unfortunately, the balloon problem is characterized by several high gradient regions, where the variables are changing rapidly, such as ascent, sunrise, and sunset, and some low gradient periods, such as night float. A time step adequate for one region would be either computationally inefficient or inaccurate in the other. Thus, the present model uses a variable time step dependent upon the current conditions.

Rigorous numerical studies with the present program and others indicate that the best approach to controlling the time step is to place limits on the maximum change each major dependent variable can have over a time step. If these tests are successfully satisfied for three consecutive time steps, the time increment is doubled. More frequent doubling is computationally inefficient. If at the end of a step or at any time during the Runge-Kutta process any one of the limits is exceeded, the step is repeated using one-half

the initial time increment. This procedure is used in the present numerical code.

Now the actual values of the variable limits can only be determined through systematic numerical studies. Based upon such studies conducted with the present code for realistic flight cases, the following limits have been selected:

$$\begin{aligned} &\left|\Delta T_g\right|_{max} < 1°K \\ &\left|\Delta T_f\right|_{max} < 1°K \\ &\left|\Delta z\right|_{max} < 50 \text{ meters} \\ &\left|\Delta (dz/dt)\right|_{max} < 25 \text{ meters/min} \end{aligned} \tag{48}$$

In addition, it has been found that time steps smaller than 10^{-5} minutes usually indicate serious input errors. Thus, the code automatically stops if such a time step is required. Further, excessively large time steps frequently lead to repetitive doubling and halving, which is inefficient. Thus, the maximum time step is limited by an input variable, DTMAX.

This value is normally defaulted to five minutes. However, if the flight involves valving periods of short duration, DTMAX needs to be set to about half the minimum valving period. This action is required since the change in mass of gas is not limited by Eqs. (48).

Another item of concern in any numerical solution is the possible error associated with cumulative significant digit and round off error. Since the present results were all obtained on the TAMU/TEES Amdahl 470/V6-7 machines, which, like all IBM type machines, only utilize seven significant digits in single precision, this possibility has been investigated. Several double precision (16 digits) arithmetic calculations have been performed and compared to their single precision counterparts. In addition, several runs were obtained using maximum time steps of about one second. In all

cases, the differences in results were insignificant. Since almost all computers utilize at least seven significant digits in single precision and many use 16 digits, single precision arithmetic should be adequate for almost all calculations.

Another factor affecting the quality of the results obtained with the model is the input data. Quite obviously correct values must be used, and in a post flight analysis accurate values for weights, ballasting, etc. are usually known. If, however, the model is used for a pre-flight prediction, many quantities may only be known approximately; and in that case the user should make a series of calculations bracketing the possibilities in order to obtain an idea of the possible flight performance.

Possibly the most important parameter affecting the ascent trajectory of a balloon is the initial mass of gas. Initial attempts to simulate actual flights with the present model were unsatisfactory in that the predicted ascent velocities above the tropopause were too low. Subsequently, a sensitivity analysis was conducted to determine which parameters affect this region; and it was determined that the most important quantity was the amount of lifting gas.

Consequently, the inflation computation sheets were obtained from the flight records of several flights; and, using the charts and procedure outlined in Ref. 31, the amount of gas put into the balloon was computed. Consistently, this approach has yielded a mass of gas about three percent higher than that determined from the assumed free lift; and theoretical results obtained using this extra gas are in excellent agreement with flight trajectories. Consequently, in using the present model it is recommended that the initial mass of gas be three percent above the value determined from the specified free lift.

Now this need of the present model for extra gas should not be construed as a criticism of current launch procedure or launch operations personnel. Their excellent performance record is undeniable, and they have consistently launched balloons which accurately meet the performance criteria of the user. Perhaps, the explanation is simply that there is an erroneous assumption in the present theoretical model. On the other hand, the tables in Ref. 31 are slightly different from those actually used by the inflation crews; and the fill procedure of an inflation period, followed by a wait for pressure gages to adjust, another inflation period, etc., should always result in a slight extra amount of gas being placed in the balloon. In any event, operational procedures should remain unchanged and the present model should probably assume three percent extra gas.

At float, an important parameter affecting model accuracy is the maximum balloon volume. In general, use of the manufacturer's specified volume in the model has resulted in accurate prediction of float altitude. In two cases, however, slightly smaller volumes had to be used. Since float volume can accurately be determined from ambient and gas conditions and the mass at float, it is obvious for these cases that the float volumes are wrong. Since some manufacturers do not use sophisticated computer codes and design balloons based upon sigma tables, the occasional existence of a small volume error is not surprising. Consequently, the user of the present model and code should always keep this possibility in mind when evaluating his theoretical results.

Finally, some comment should be made concerning the overall accuracy of the present model. It is believed by the present investigators that this model will, when used with accurate and appropriate input data, yield accurate results. However, one of the primary governing parameters is local free lift.

$$\text{FreeLift} = \rho_a V - m_{total} \tag{49}$$

For large balloons, $\rho_a V$ and m_{total} are very large in magnitude and free lift is very small. Thus, some significant digit loss will occur in the computation of free lift. Hence, the present model should be slightly less accurate for large systems than for small balloons.

V. TYPICAL RESULTS

In this section, typical results obtained with the present model and computer program will be presented for several balloon flights. These results will be discussed and compared with actual flight data. In addition, the results of pertinent sensitivity studies of various flight parameters will be presented where appropriate.

Figure 3(a) and 3(b) show trajectory results for the RAD I flight. RAD I, or flight 913 PT, was an engineering test flight of a 56634m^3 balloon and was launched at about 0130CST on 29 August 1975. As can be seen, the agreement between the theoretical trajectory and the measured one is excellent, particularly in the vicinity of the tropopause. Upon arrival at float, the theory shows that the balloon went through several vertical oscillation in the process of expelling or "burping" gas before settling down to a steady float altitude. The actual balloon descended slightly shortly after float, possibly due to a small decrease in the earth-air infrared input not accounted for in the theory. This difference in altitude, about 500 meters, was maintained throughout the night.

Figure 3(b) shows the trajectory during sunrise, which started at 251 minutes, and the daylight portion of the flight. The altitude increase at 243 minutes is due to a 13.62 kg ballast drop, and the oscillations shortly thereafter are a consequence of sunrise and the resultant gas heating and additional gas expulsion. This agreement between theory and experiment is

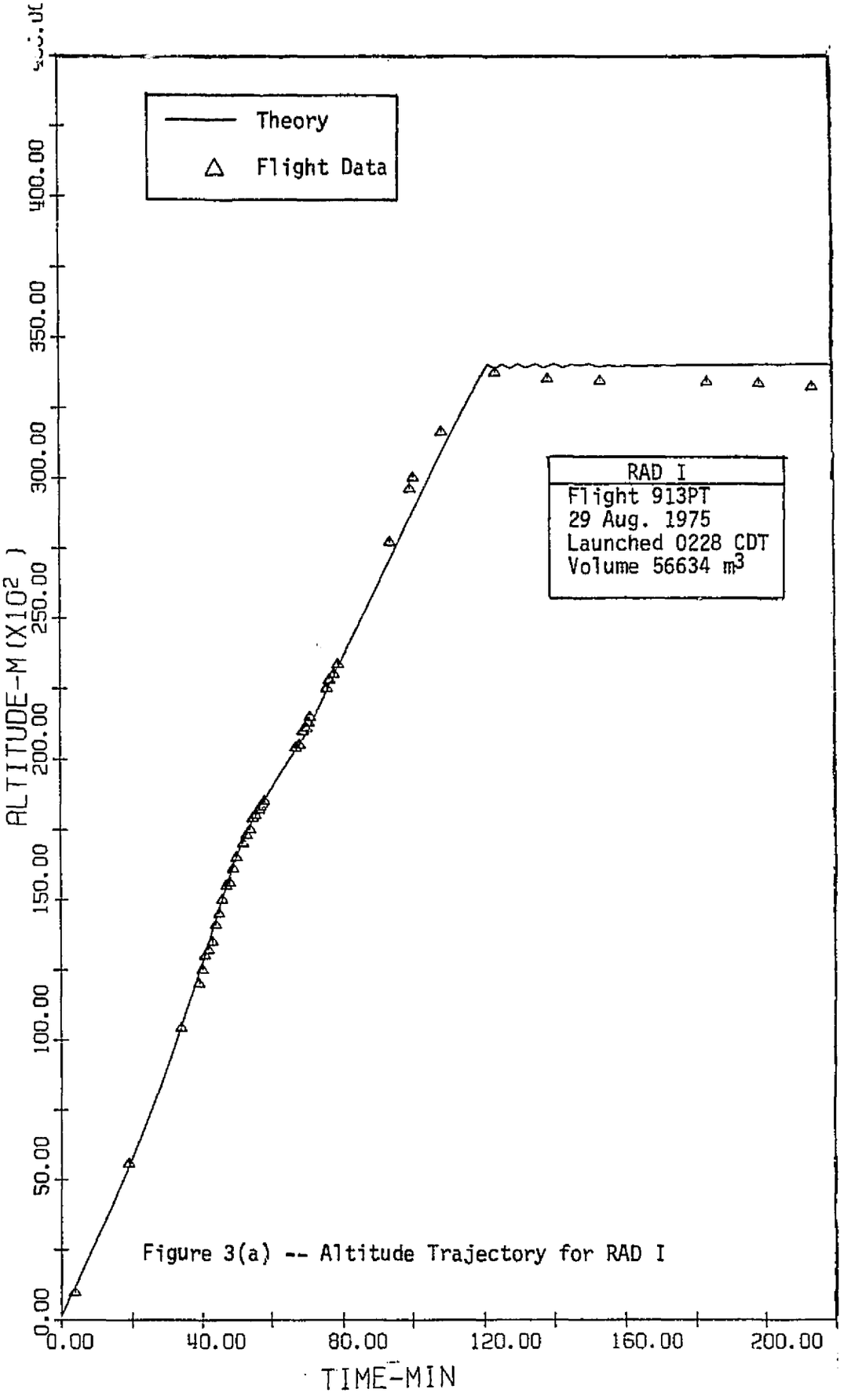

Figure 3(a) -- Altitude Trajectory for RAD I

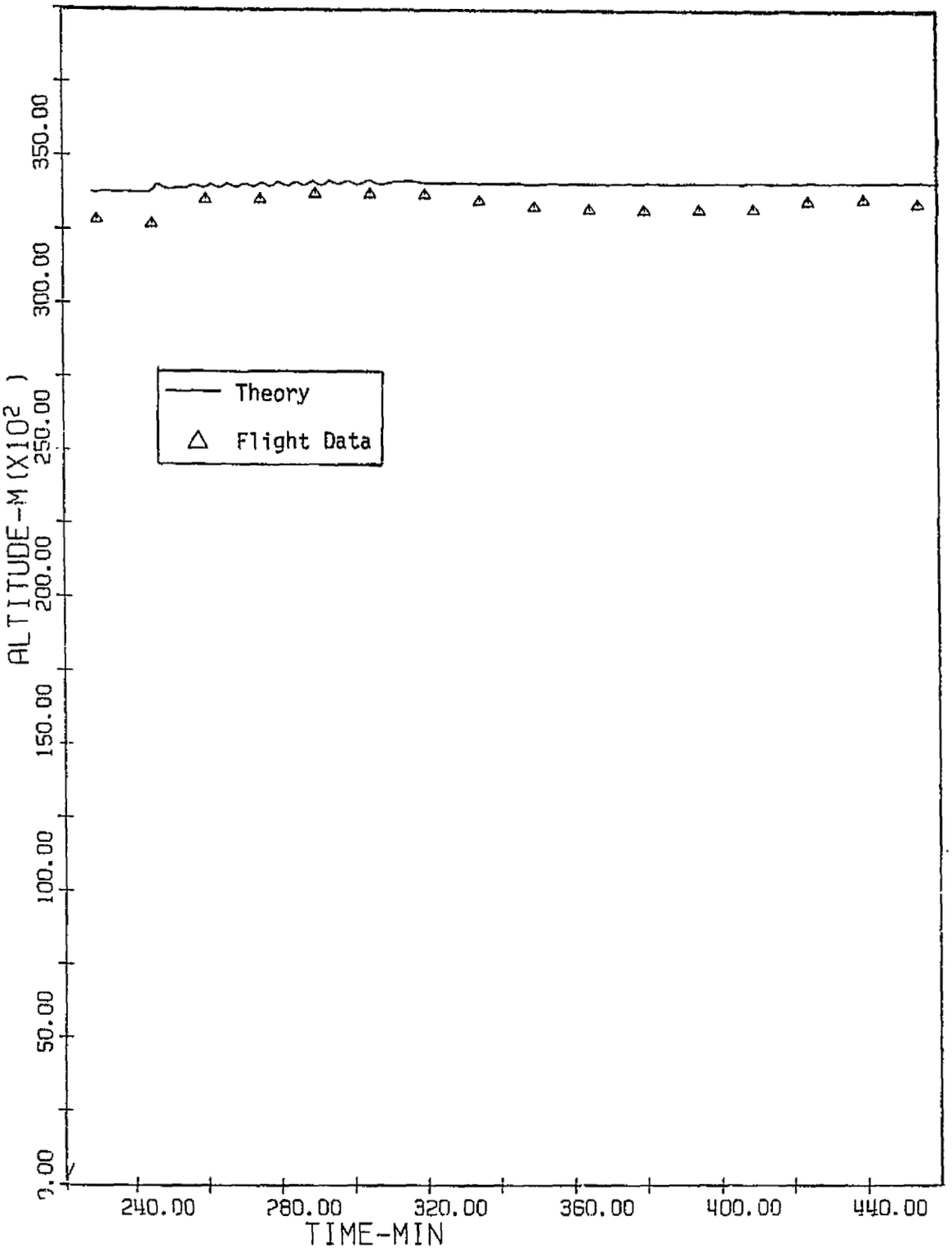

Figure 3(b) -- Altitude Trajectory for RAD I

good, particularly considering the fact that the experimental altitudes were obtained using the 1962 standard atmosphere. As mentioned previously, such a data reduction procedure can lead to altitude errors up to 500 meters.

Figures 4(a) and 4(b) show similar comparisons for the temperatures. On this flight, only gas temperatures were measured; and only the data measured by the upper thermistor are plotted. In general, the agreement is excellent. During ascent, and particularly after the tropopause, the gas temperature is lower than that of the film due to the effects of adiabatic expansion cooling. The slight decrease in gas temperature at 69.6 minutes is due to a 13.62 kg ballast drop. Ballasting almost always induces a sudden increase in ascent rate and creates a temporal increase in adiabatic cooling. Thus, gas temperature is a sensitive indicator of the effects of ballasting.

Float, here defined as when the balloon first vents gas, was achieved at 122 minutes. As can be seen on Fig. 4(a), the gas temperature subsequently took about thirty minutes to increase to its equilibrium float value. The oscillations during this period are due to the balloon oscillating about its nominal float altitude, expelling gas, and undergoing cyclic adiabatic expansion and compression.

Since this balloon floated at night, the equilibrium gas and film temperatures should theoretically be the same. It should be noted that this equivalence did occur and that the theoretical gas temperatures agree well with the measured values. The latter is very significant since this is the first time such agreement has been achieved in a theoretical model actually using experimentally measured radiative properties of the balloon film.

Figure 4(b) presents the theoretical and measured temperatures during sunrise and the daylight portion of the flight. As shown, sunrise causes the gas temperature to increase, followed by the film temperature. This

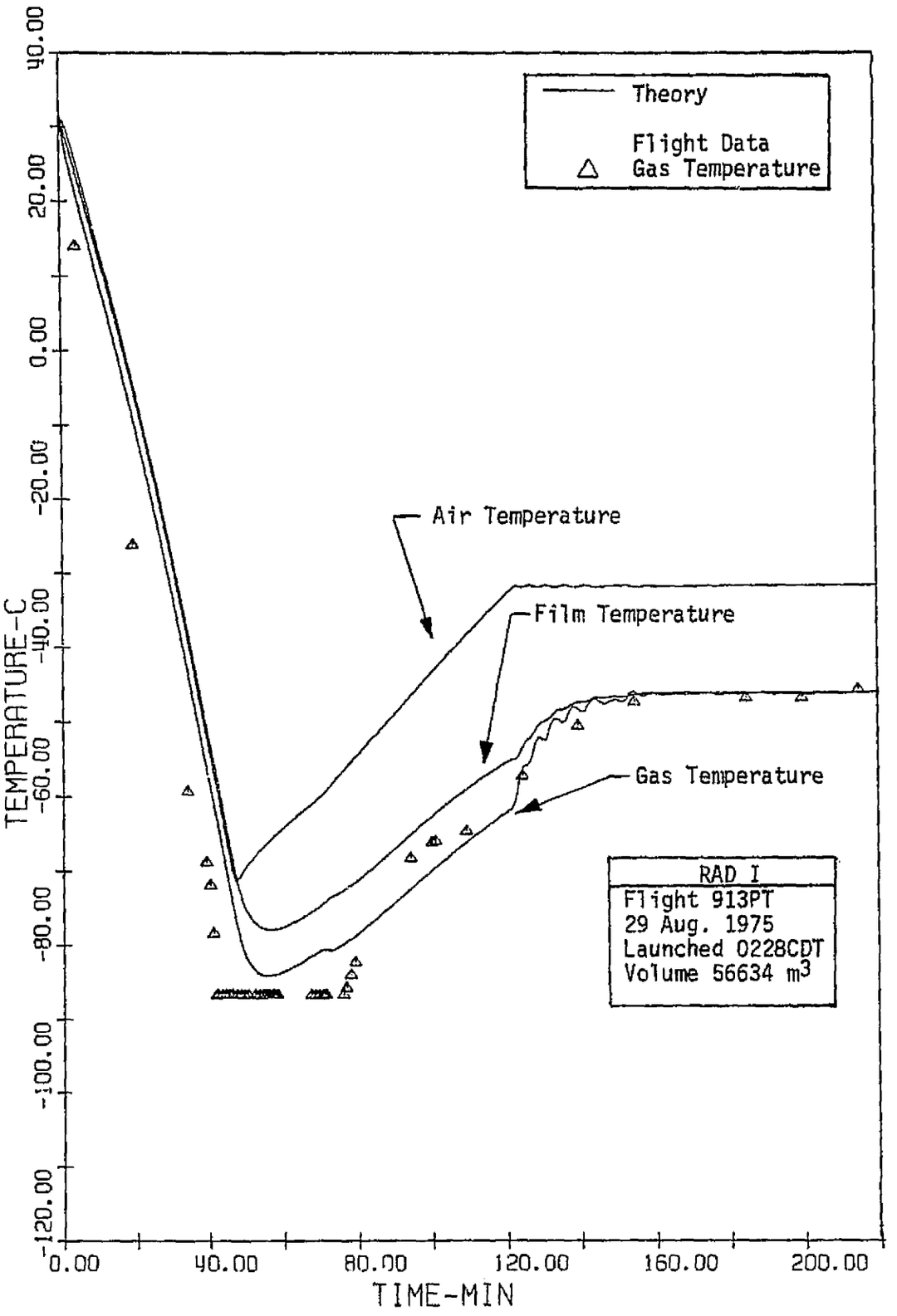

Figure 4(a) -- Temperature Profiles for RAD I

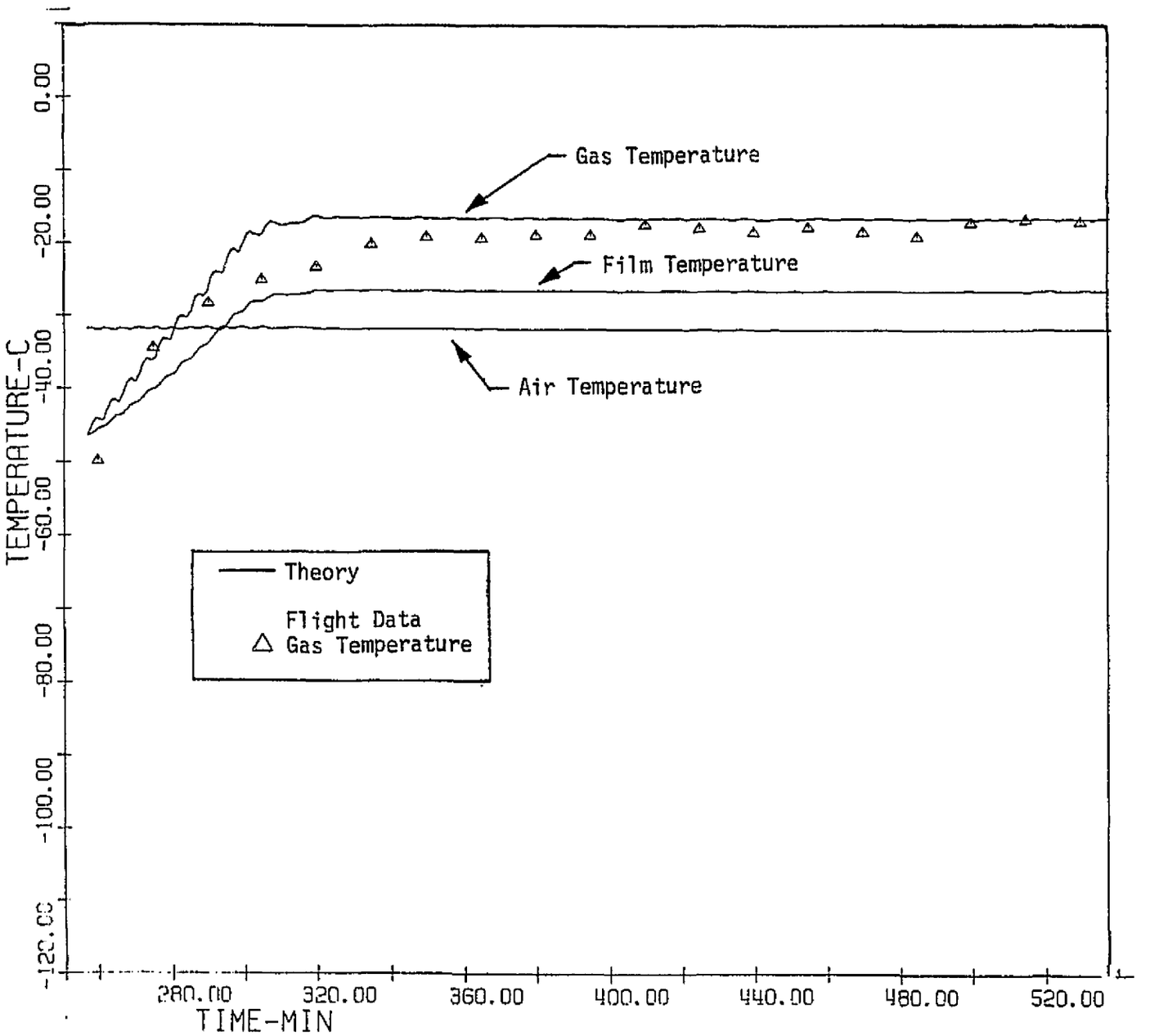

Figure 4(b) -- Temperature Profiles for RAD I

pattern is expected since the low solar absorptivity of the film would only create a slight film temperature change, and any significant increase would have to be preceded by an increase in gas temperatures. The sinusoidal behavior of the gas temperature during this sunrise period is again due to balloon oscillation and gas expulsion. The latter occurs because as the balloon heats, the mass of gas which can be contained in the balloon volume decreases.

It should also be noticed on Figure 4(b) that the daytime equilibrium gas temperature is in excellent agreement with the experimental values and is about 10°C above the predicted film value. The latter is in sharp contrast to previous theories which assume that the two temperatures would be the same. Finally, notice that the day gas temperature is about 25°C above the local ambient temperatures.

Comparisons between theory and experiment are shown for the flight of RAD III on Figures 5-7. RAD III was launched at sunset on 11 August 1976 as flight 979 PT and was a 14160m^3 balloon made of X-124 film. It was instrumented to measure gas, film, and blackball temperatures. Figure 5(a) compares the theoretical and actual altitude trajectories and shows the same characteristics exhibited by RAD I. In general, the agreement is excellent. While not shown on a figure, the actual balloon did reascend to the theoretical float altitude after sunrise, indicating that the night IR input was slightly less than assumed in the latter part of the night.

Figures 6(a) and 6(b) compare the theoretical and measured temperatures. During ascent, the theoretical gas temperatures again exhibit adiabatic cooling; and the agreement with the measured values is surprisingly good. The gas temperature pause at 82.3 minutes is due to ballast drop, and the night float temperature show good agreement with the theory. As can be seen, the gas and film values are very close to ambient, probably because this

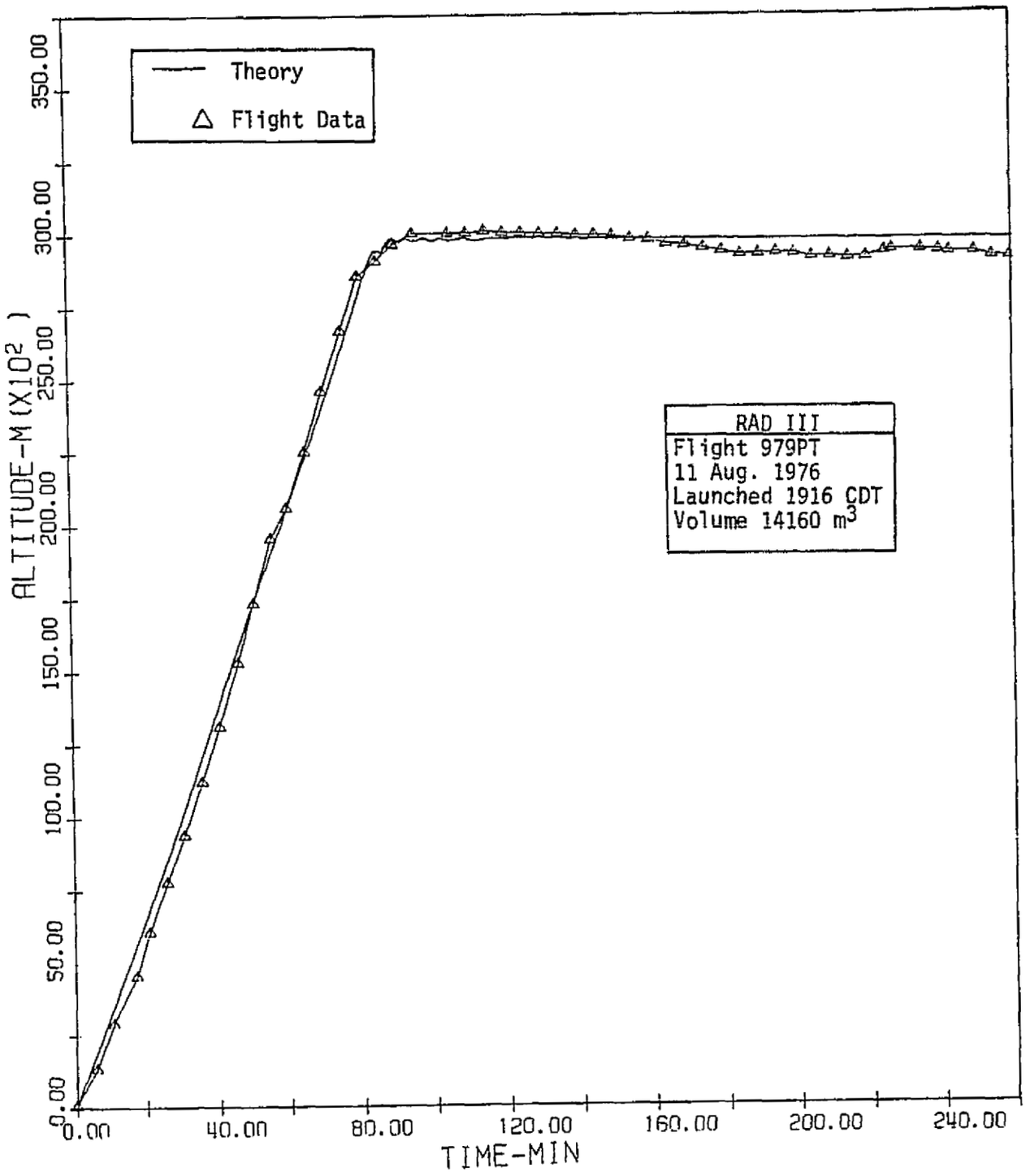

Figure 5 -- Altitude Trajectory for RAD III

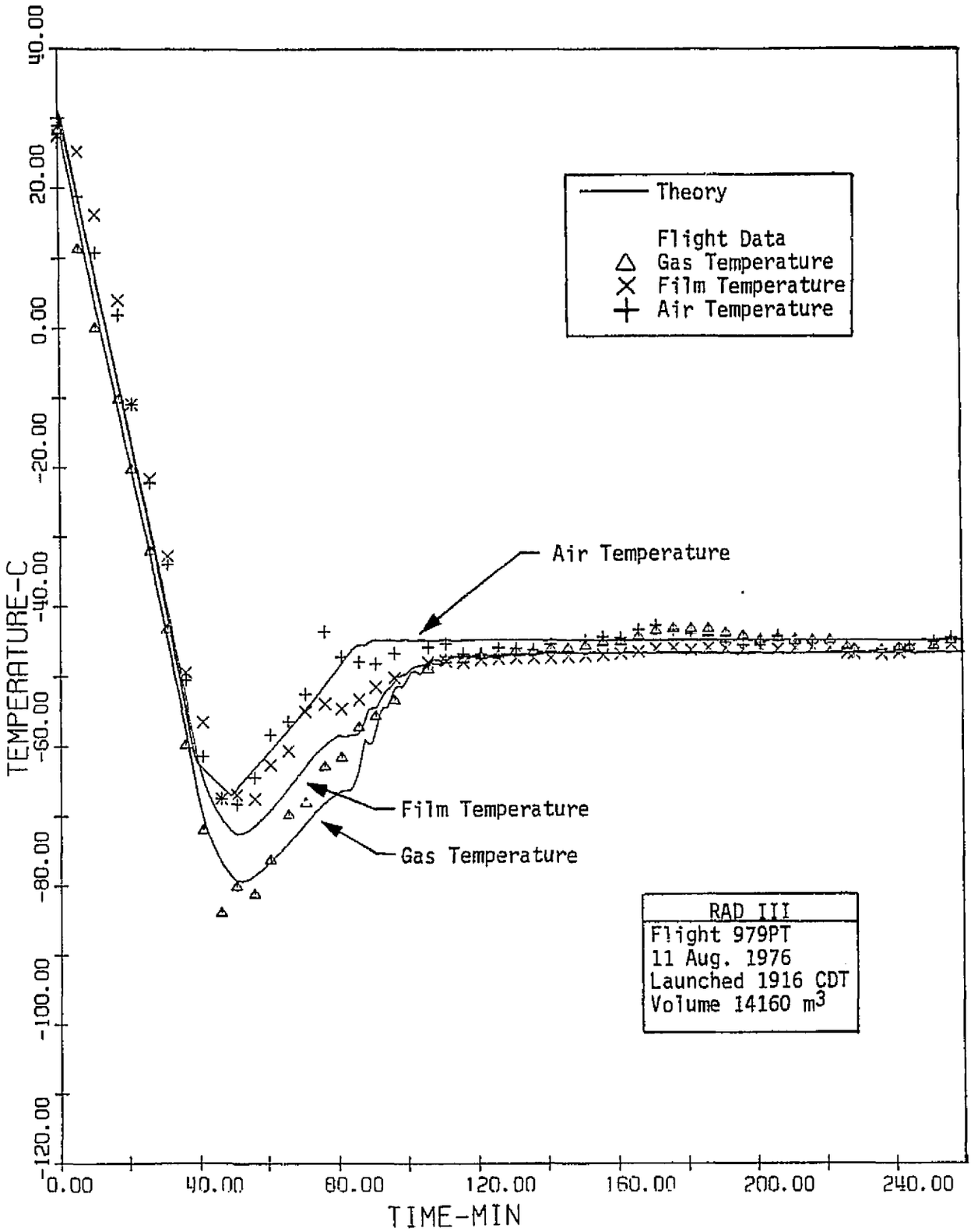

Figure 6(a) -- Temperature Profiles for RAD III

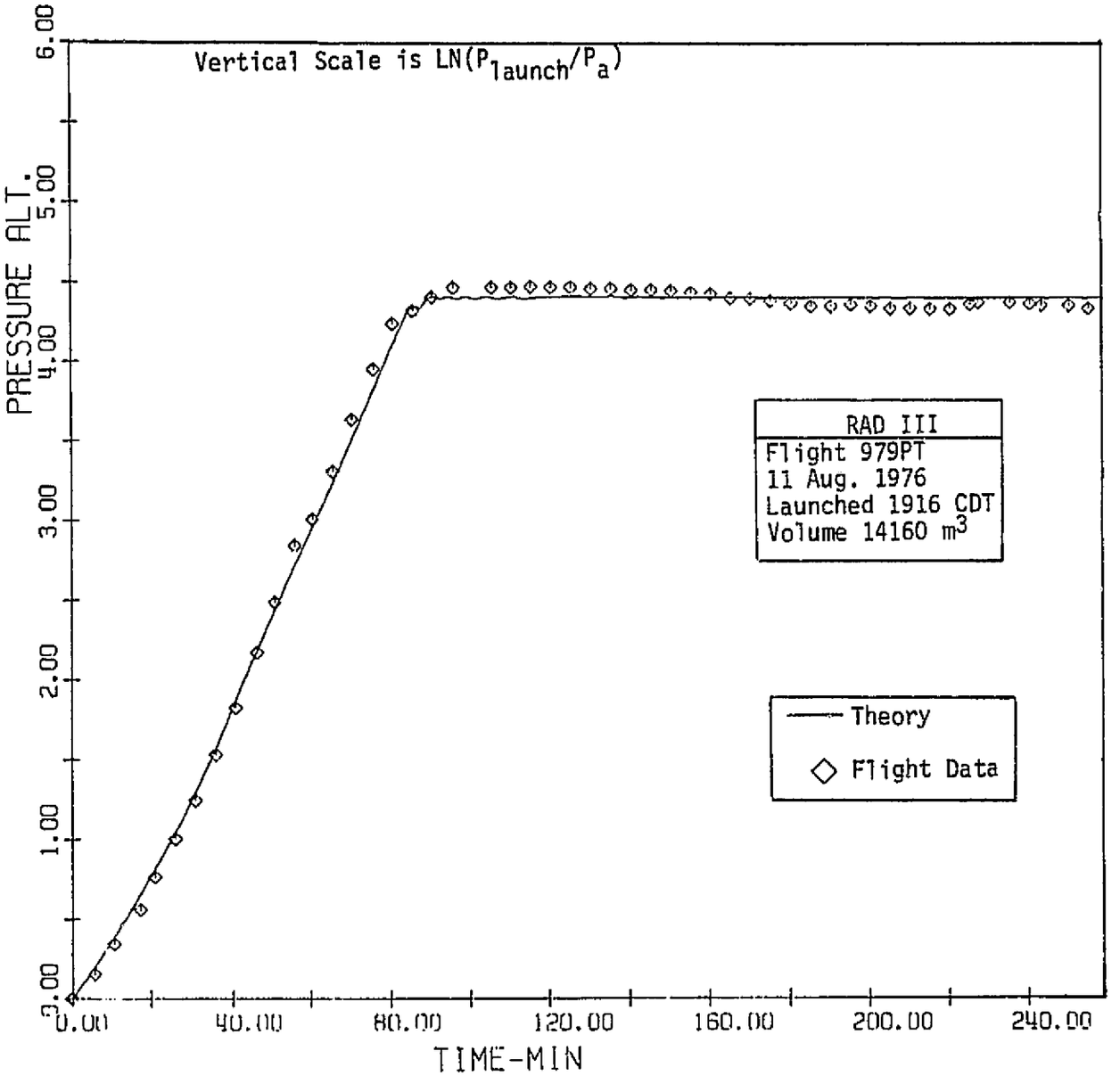

Figure 7 -- Pressure Trajectory for RAD III

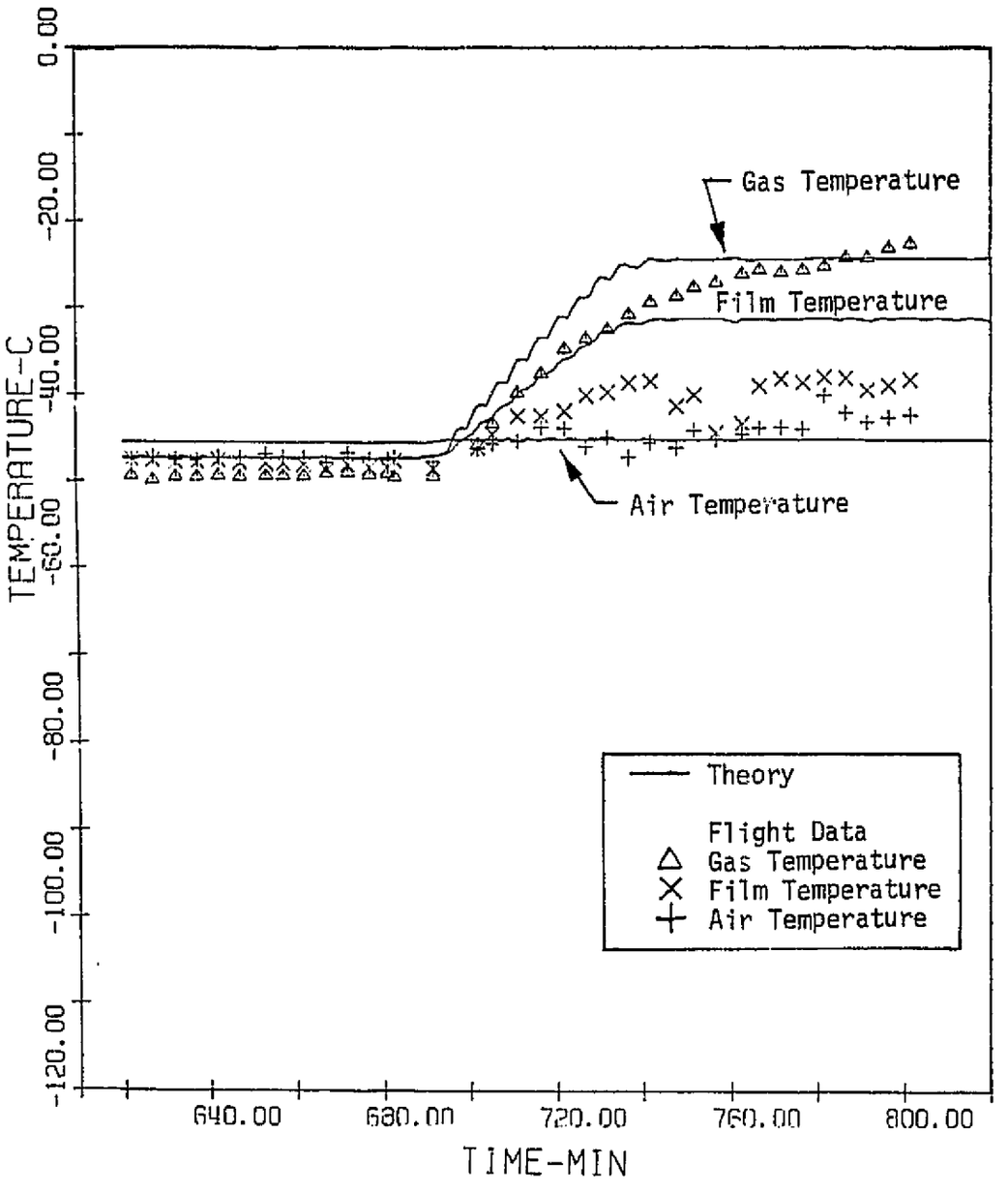

Figure 6(b) -- Temperature Profiles for RAD III

summer flight experienced an unusually high blackball input of 225K. The usual value is 214.4°K.

The thermal behavior of RAD III during sunrise is shown on Figure 6(b), and the agreement between theory and experiment for gas temperature is considered acceptable by the present investigators, particularly near the end of the flight. The theoretical and experimental film temperatures, however, disagree after sunrise. This difference is not surprising since the theoretical model used film radiative properties for Stratofilm.^{R} X-124 film has a different molecular structure, and based upon the present results probably has a slightly lower solar absorptivity. Since present balloons are made from Stratofilm^{R} and X-124 is no longer manufactured, this discrepancy is not considered significant.

Now in comparing theoretical and experimental balloon trajectories, atmospheric pressure versus time should be used rather than geopotential altitude, since pressure is the quantity actually measured in an instrumented flight. This approach eliminates discrepencies which may result when an altitude is determined from a measured pressure and the 1962 Standard Atmosphere and the actual altitude profile differs from the standard. Such a pressure comparison is shown on Figure 7 for RAD III. Here, and on all pressure plots in this report, the vertical scale is $\log_e (P_{launch}/P_a)$. Since the atmosphere is almost exponential in nature, such a scale yields curves which look similar to an altitude plot. As can be seen, the agreement is excellent.

As discussed in this and previous sections, RAD III encountered an unusual atmospheric profile, particularly with respect to blackball temperatures. Thus, it should serve as an excellent vehicle for studying theoretically the sensitivity of the predicted results to different atmospheric

assumptions. Figure 8 portrays the pressure trajectory for RAD III computed using the Palestine, TX standard summer profile and compares it to the actual flight data. For this case, the standard blackball profile was also used. Below the tropopause, the agreement is good but above it the two results differ, and the theoretical float altitude is slightly lower than that shown on Fig. 7.

Figure 9 compares the corresponding temperature profiles, and during ascent the agreement is probably acceptable. However, the predicted float temperatures for this summer atmosphere are about 3°C below those previously predicted on Fig. 6(a). Thus, the usage of a summer atmosphere for this flight leads to some trajectory and temperature errors. These differences might, however, be acceptable in many cases.

Figure 10 compares similar theoretical results obtained using a 1962 Standard Atmosphere. The use of such a profile is readily apparent in the essentially constant ambient temperature region in the vicinity of the tropopause. For this case, the flight trajectory is almost identical to that of Fig. 9; and thus, it is not shown separately. The predicted temperatures shown on Fig. 10 are, however, significantly different from both the flight data and the theory on Fig. 6(a). At launch, the initial temperatures differ by about 13°C, and the standard atmosphere results completely miss the minimum gas temperatures encountered at the tropopause. Notice that the constant ambient tropopause creates essentially constant gas and film temperatures for about thirty minutes of the flight. In addition, the float temperatures differ significantly from those actually measured. Based upon these results, it is concluded that the use of the 1962 Standard Atmosphere in predicting and analyzing balloon flights can lead to significant errors.

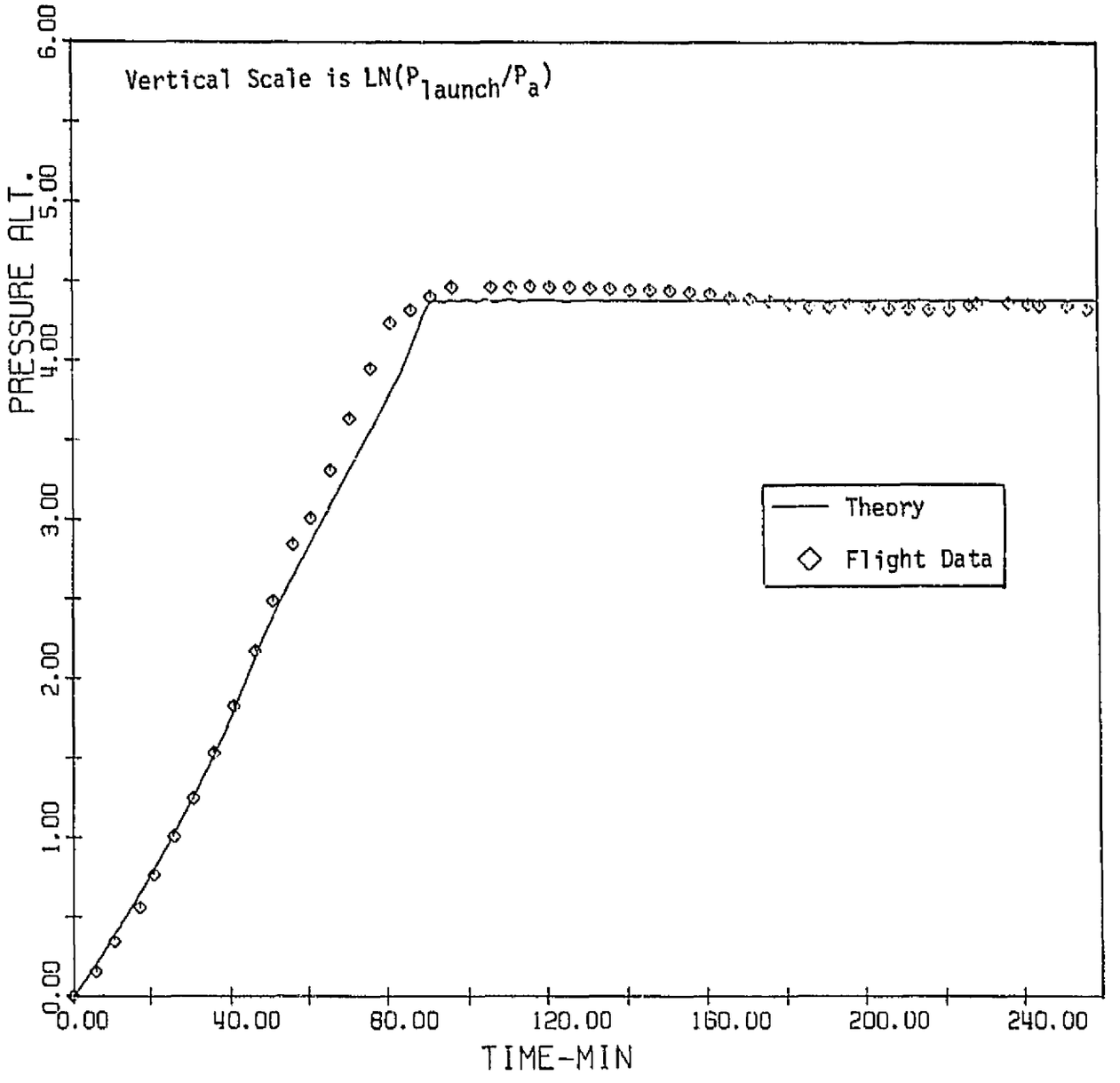

Figure 8 -- Pressure Trajectory for RAD III, Summer Atmosphere

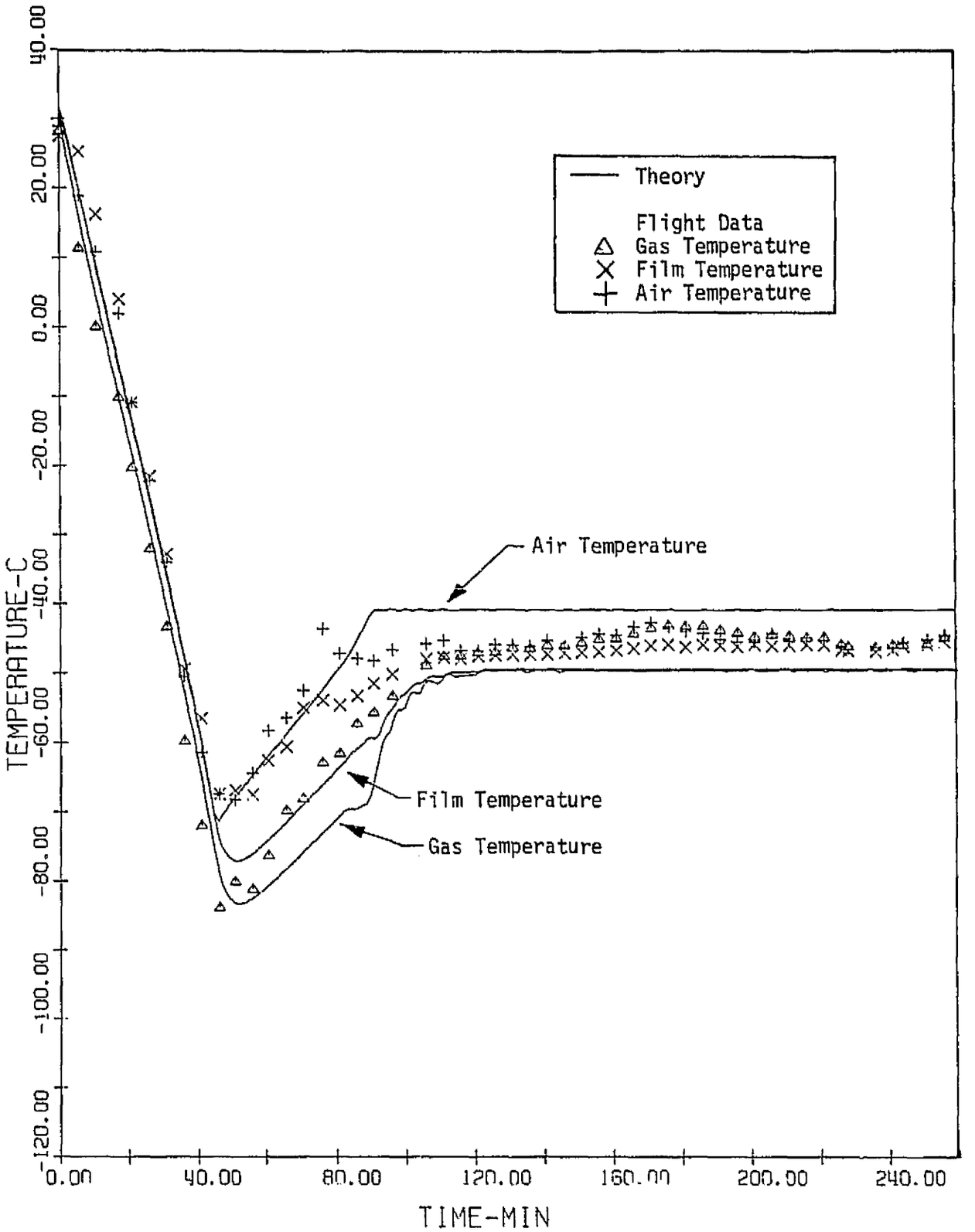

Figure 9 -- Temperature Profiles for RAD III, Summer Atmosphere

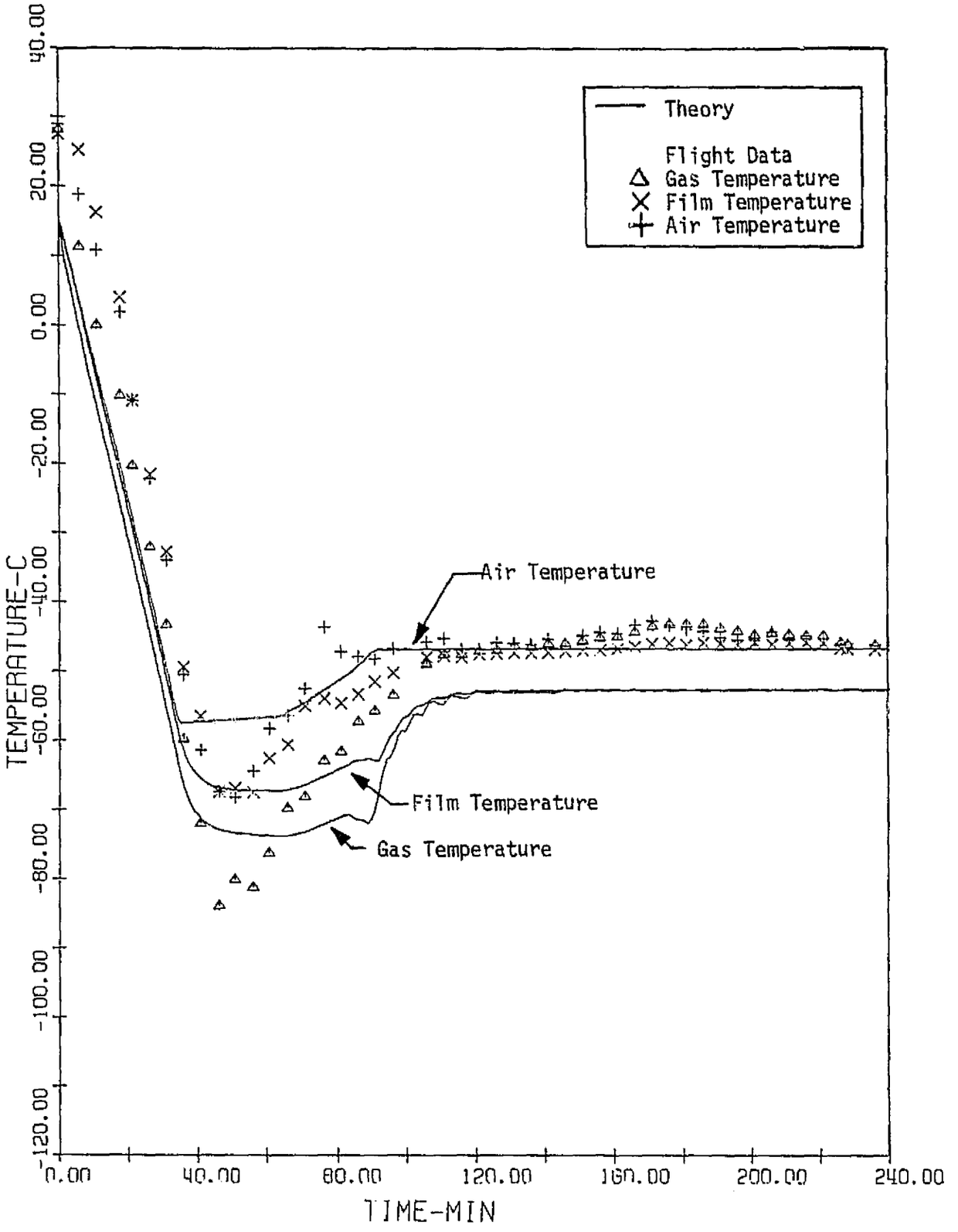

Figure 10 -- Temperature Profiles for RAD III, Standard Atmosphere

Now the present program and method should also be applicable to large balloons and daylight launches, and Figure 11 shows trajectory results for such a case. This flight, No. 1116PT, used a large 965,326m^3 balloon and was flown on 10 December 1978 at 1022 CST. This flight was part of the heavy load study program;[12,25] and was terminated shortly after arrival at float.

For lack of better information, the simulation of this flight used a standard Palestine winter atmosphere; and only an altitude plot is shown since the pressure plot is similar. In general, the agreement with flight data is good with the possible exception of the entrance into float. This flight is unusual in that it had fourteen ballast drops, with about half of these occurring after arrival in the vicinity of float. Consequently, both the theory and the flight data exhibit a gentle increase in altitude in the last portion of the flight. The discrepency in float altitude may be due to an error in the ballast history or the assumed atmospheric profile. In addition, this flight was instrumented with a gas temperature thermistor. However, a single thermistor, based on other flights, may not be representative of the average gas temperature. Consequently, temperature profiles are not shown since they are similar in character to those previously discussed. In any event, the results on Figure 11 indicate that the present method can be successfully applied to large balloons.

Another flight in the Heavy Load Test Program that is of interest is 1131P. This flight occurred on 12 April 1979 and used a 1,174,000m^3 balloon launched at sunset. While the initial portion of this flight appeared normal, the balloon catastrophically failed upon arrival at float. Consequently, it was decided to analyze this flight in an attempt to determine if there was anything unusual about its performance.

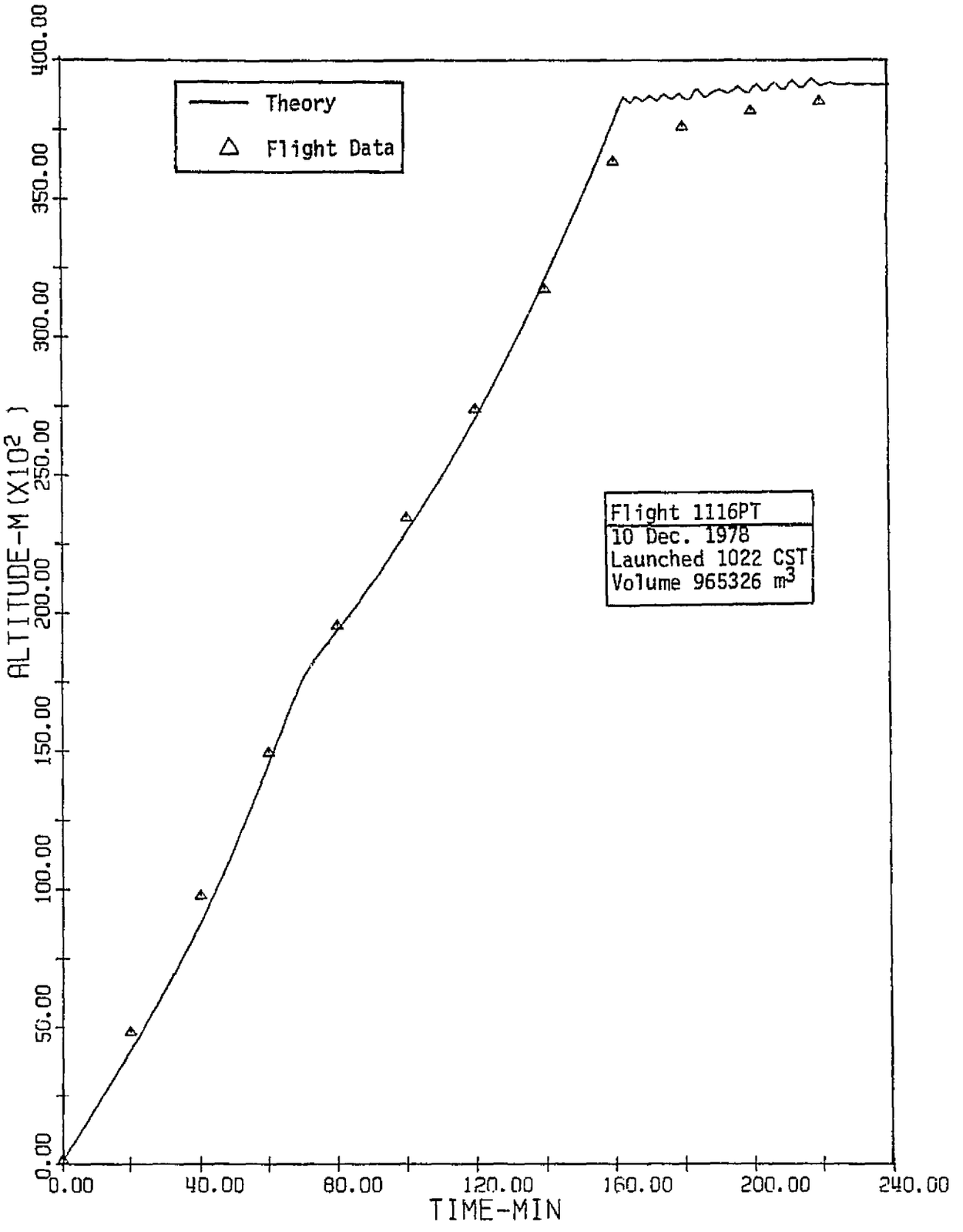

Figure 11 -- Altitude Trajectory for Flight 1116PT

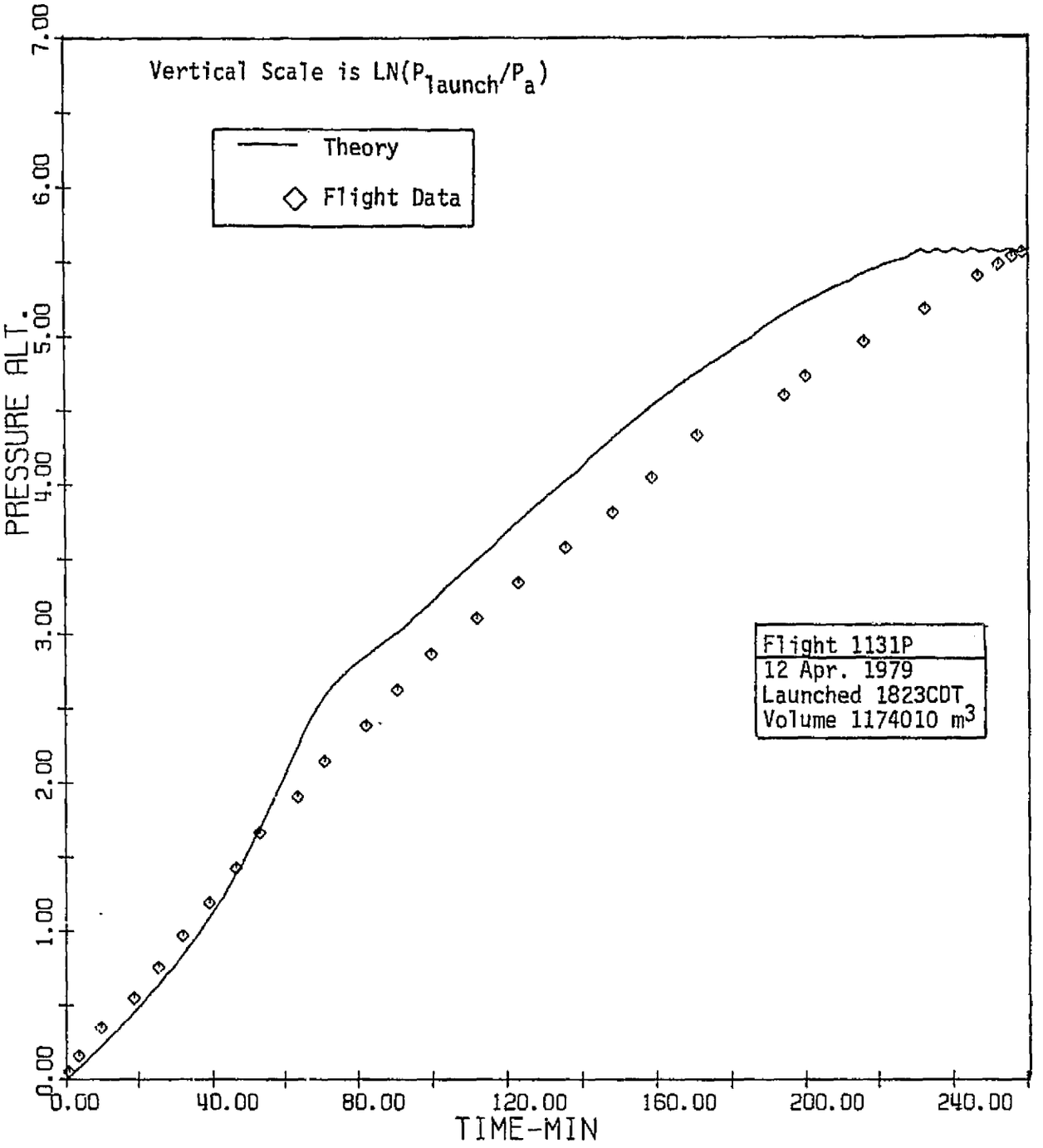

Figure 12 -- Pressure Altitude Trajectory for Flight 1131P

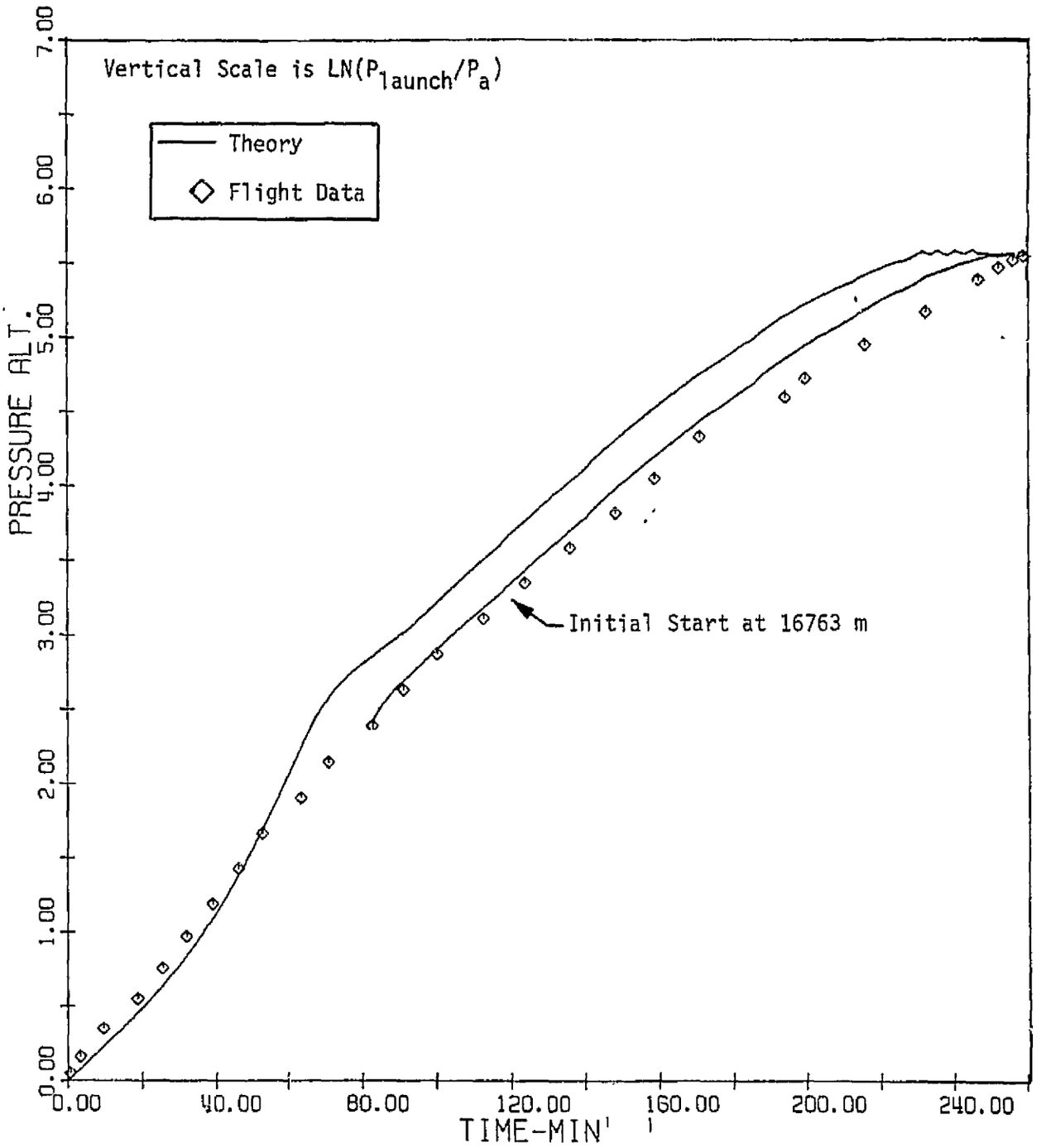

Figure 13 -- Pressure Altitude Trajectories for Flight 1131P

Pressure trajectory results for this flight are shown on Figure 12, and below the tropopause the theory is acceptable considering that it used a standard Palestine spring atmosphere profile. Above the tropopause, the theoretical trajectory appears to have the correct slope, and the final float altitude agrees with the flight data. However, there are significant differences between the theoretical and actual results in both magnitude and character in the vicinity of the tropopause.

Subsequent study of the flight records, which contained a limited amount of air thermistor data, revealed that between about sixty and eighty-five minutes after launch the balloon encountered several temperature inversion layers. Within these layers air temperature variations of 15 to 25°C were rapidly encountered; and the balloon velocity varied considerably. In addition, the theoretical results predict for this period gas temperatures of -92°C and average film temperatures below -83°C, which are significantly colder than those predicted for other night flights. Now the cold brittle point of polyethylene is about -80°C. Since some parts of the film may have been colder than the average and since two 32.7 kg ballast drops occurred during this period (at 58.2 and 68.7 minutes), there exists the possibility that the balloon film sustained damage, weakening, or even failure during this period.

If any film failures did occur near the tropopause, they should affect the subsequent trajectory. To investigate this possibility, results have been obtained with the present method using for initial values the flight conditions at 82.25 minutes after launch. The resultant profile, as well as the original one and the flight data, is shown on Figure 13. As can be seen, the agreement is relatively good; although there is some divergence after 180 minutes, possibly due to atmospheric effects. Thus, it appears from

these results that the balloon did not experience shell failure while traversing the unusual inversion layers near the tropopause.

Nevertheless, it is known that 1131P underwent severe sailing and flapping during the dynamic launch period and that there was evidence of possible manufacturing or pre-launch handling film damage. When those facts are combined with the possible existence of extremely cold temperatures and velocity variations near the tropopause, it appears likely that the balloon film sustained significant and unusual weakening and straining prior to arrival at float. Quite possibly, these events led to the subsequent catastrophic failure.

Obviously, the primary objective of the present program is to develop a model and computer code capable of accurately analyzing the thermal and trajectory performance of a balloon flight. On 24 July 1980, engineering personnel of the National Scientific Balloon Facility flew RAD IV. This 66375m^3 balloon, flight number 167N, was launched during the daylight at about 1135CDT, flew through sunset, and was terminated near sunrise the next morning. It was probably the most extensively instrumented, from a thermal viewpoint, flight to date. The balloon contained five gas thermistors suspended vertically along the centerline plus two other located 14 meters outboard on the equatorial plane. In addition, it included ten film thermistors on the outside of the film and two on the inside.

Consequently, this flight has been analyzed with the present program using the model, heat transfer and drag coefficients, parameter correlations, etc. developed in the present research effort. It is believed that by comparing these results with the flight data an idea of the validity and accuracy of the present method can be obtained.

Figures 14(a) through 14(d) compare the pressure trajectory predictions with the flight data, and the agreement is generally excellent. In Fig. 14(a),

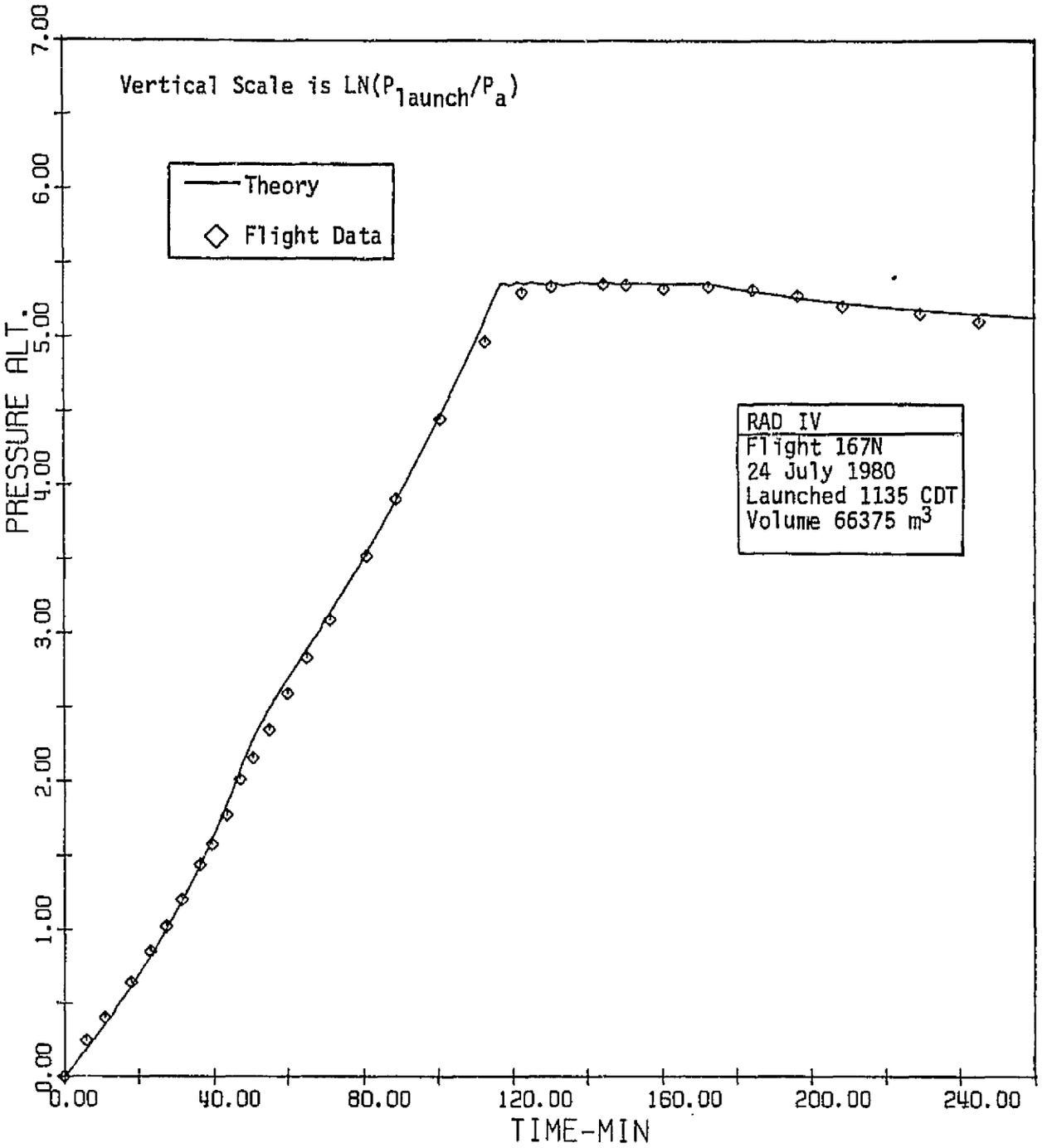

Figure 14(a) -- Pressure Altitude Trajectory for RAD IV

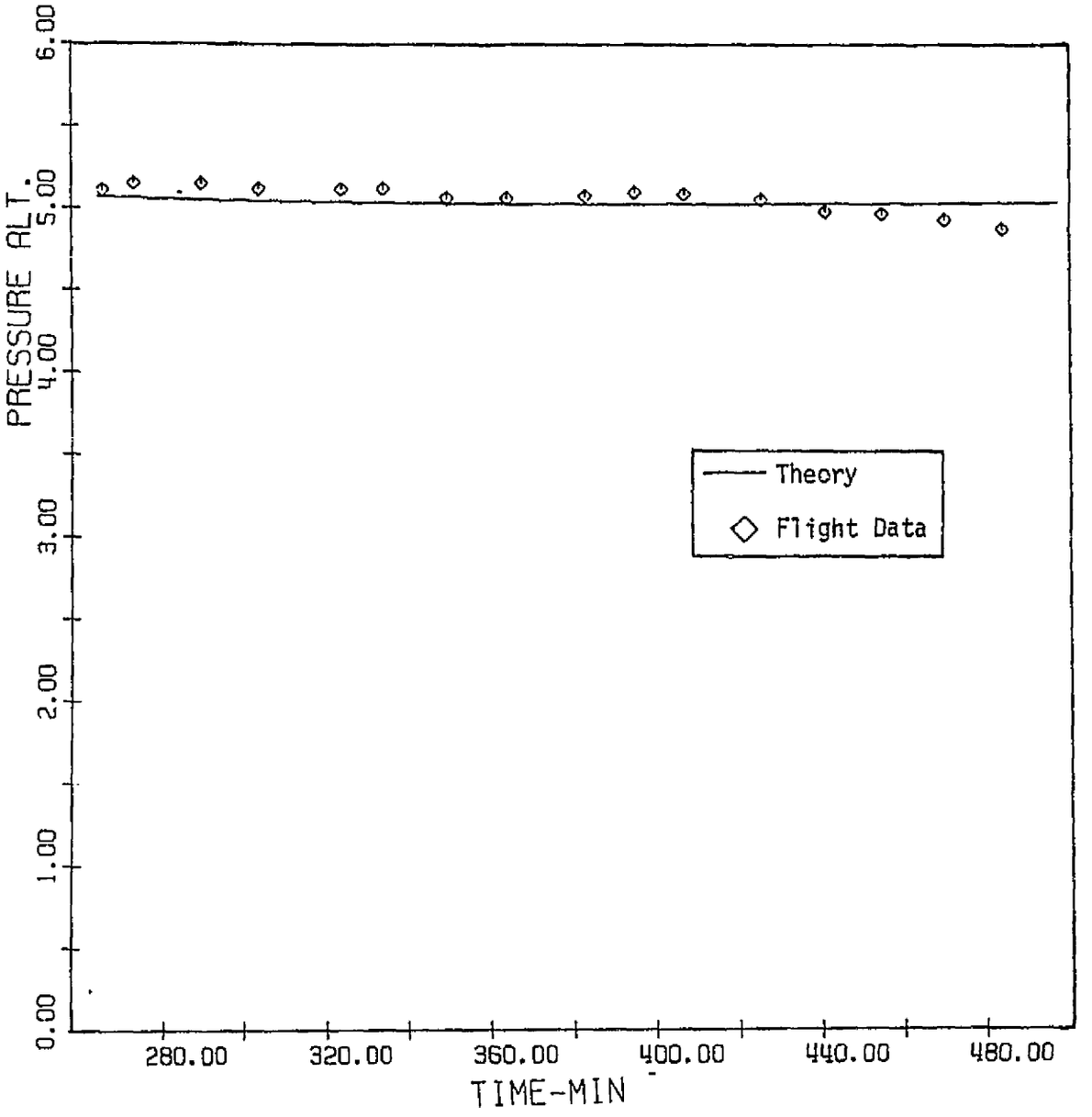

Figure 14(b) -- Pressure Altitude Trajectory for RAD IV

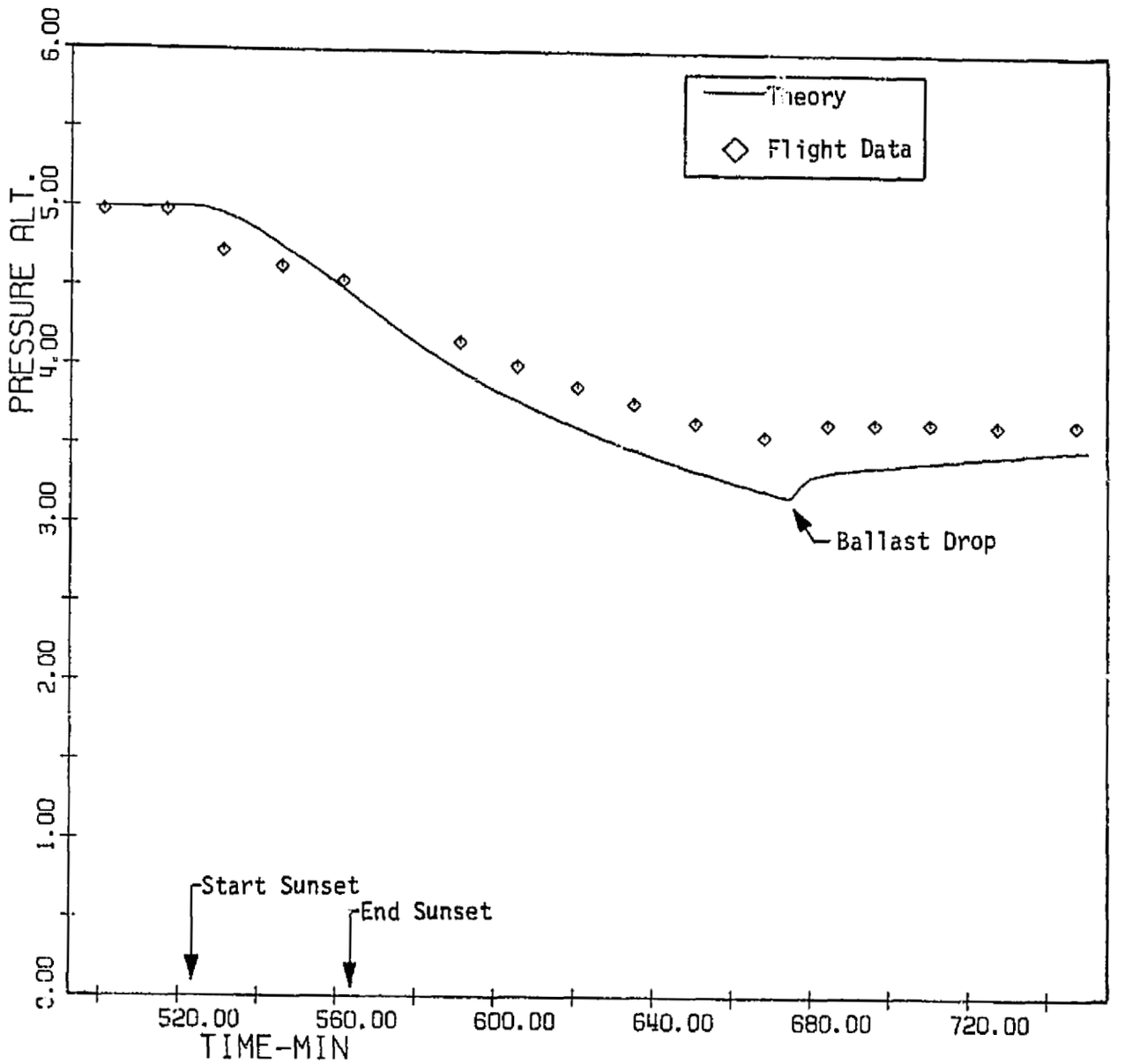

Figure 14(c) -- Pressure Altitude Trajectory for RAD IV

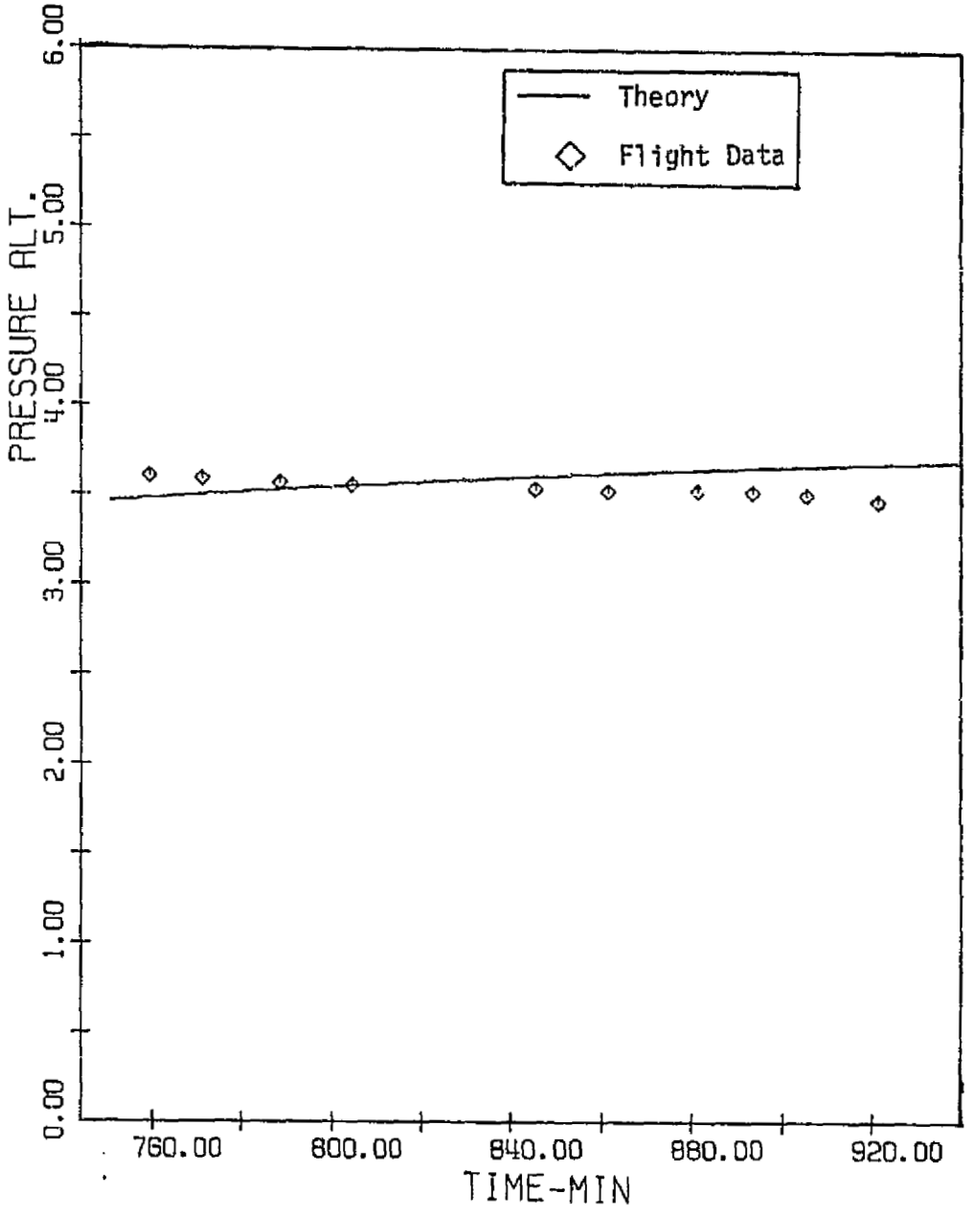

Figure 14(d) -- Pressure Altitude Trajectory for RAD IV

the effect of the balloon passing over high cirrus at 170 minutes can be seen in the onset of a gentle descent; and the model correctly predicts the trend of this effect.

However, probably the most interesting of these plots is Fig. 14(c), which shows the trajectory during sunset. While not exactly accurate, the predicted trajectory has the correct behavior. During the latter portion of sunset, the descent velocity is quite high, reaching -137 m/min, followed by an asymptotic decrease in descent rate during the night. At 673 minutes, a 22.64 kg ballast drop was executed in order to stop the descent. At this point, the descent velocity according to the theoretical model was still -43 m/min.

As can be seen on Fig. 14(c-d), this ballasting did stop the descent and result in an essentially stable float for the rest of the night in both the flight and theoretical cases. Interestingly, for the four hours following this drop the actual balloon experienced a slow descent after its initial rise, while the theory predicts a slow ascent on the order of 5 m/min.

At this point, it might be pertinent to examine the validity of the well established formula[2].

$$\text{Descent Rate} = (800 \text{ ft/min})\left(\frac{m_{balloon}}{m_{balloon} + m_{payload}}\right)(.3048\text{m/ft}) \qquad (50)$$

for estimating descent rate due to sunset. For RAD IV, this formula yields -117.9 m/min. As mentioned, the present theory predicts values up to -137 m/min. falling off to -43 m/min at the ballast drop. For the entire descent, the theoretical average is -81.5 m/min. Thus, it appears that Eq. (50) can be used to estimate the order of magnitude of the descent velocity; but it should be noted based upon both the theory and the flight data that the actual phenomena is exponential in behavior and not linear.

Figures 15(a) through 15(d) show temperature profile comparisons for RAD IV. Due to the fact that 167N was launched remotely, complete accurate thermistor data was not obtained prior to about 80 minutes into the flight; and the plotted experimental data represents the average of all pertinent thermistor readings. In general, the predicted temperatures are in acceptable agreement with the flight data, particularly during the daytime float portion of the flight. There, Fig. 15(b), the gas temperatures are accurately predicted; and the relationship between gas, ambient, and film values, with the gas highest and film coolest, is correctly reproduced.

During sunset, Fig. 15(c), and the subsequent period before the ballast drop, the difference between the predicted gas and ambient temperatures is almost constant. Interestingly, this result is in agreement with the statement of Ref. (2) that:

> "[based upon] temperature measurements, during the descent after sunset, the balloon descends at such a rate that the superheat is maintained at essentially the same value it had before descent began."

At the ballast drop, the theoretical gas temperature drops sharply due to the sudden change from descent to ascent and the resultant adiabatic cooling. As a result, the subsequent temperatures are cooler than the flight values. However, at the end of the flight, Fig. 15(d), the agreement is excellent.

While Figures 14 and 15 indicate that the present method is reasonably accurate, they do not demonstrate that it is an improvement over previous models.[4] Such models assume that the lifting gas is radiatively inactive, and this situation can be duplicated in the present version simply by setting α_g and ε_g equal to zero. Results for such an assumption are shown for RAD IV on Figures 16 and 17, and they should be the same as those which would be obtained using the method and code of Ref. (4). As can be seen

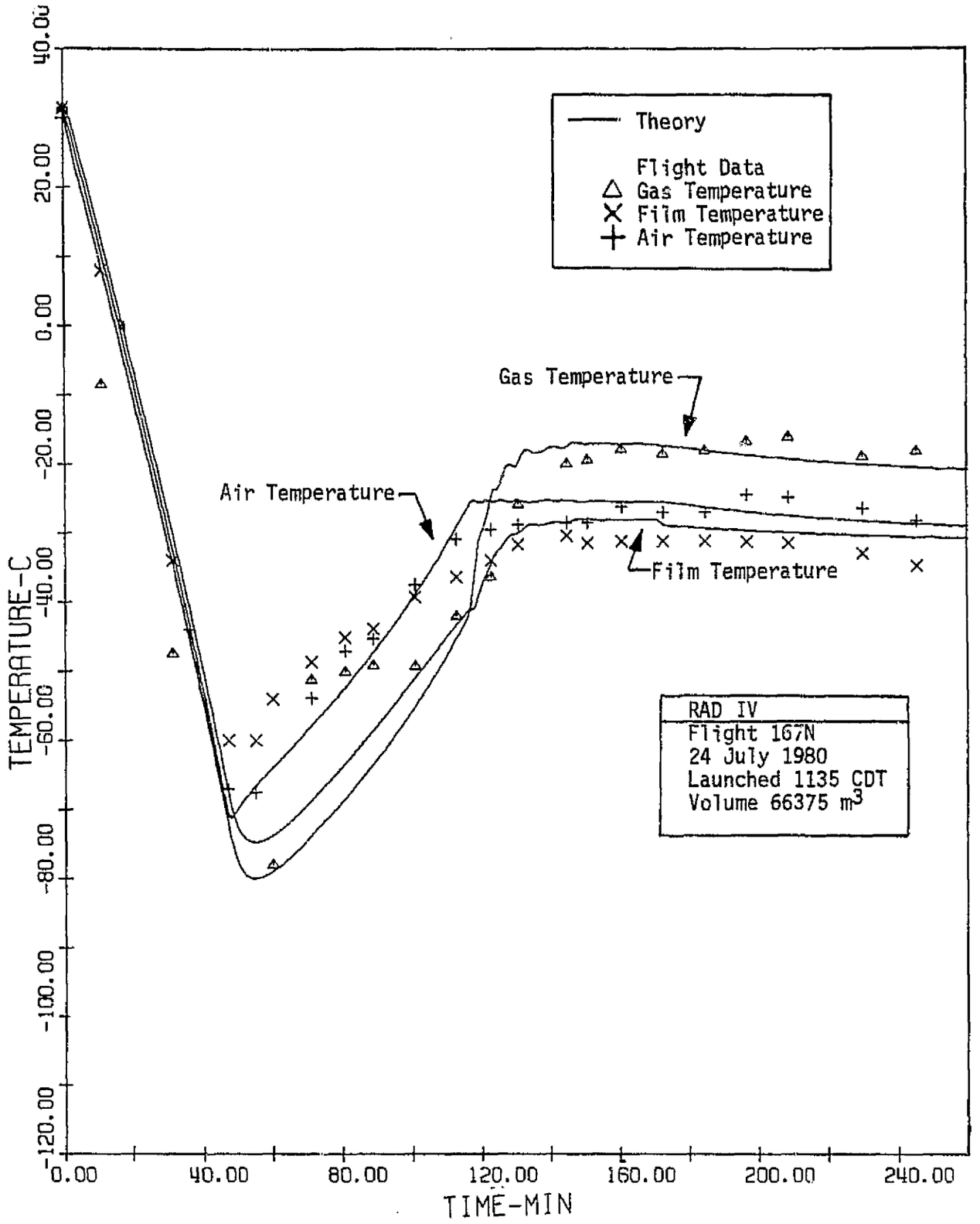

Figure 15(a) -- Temperature Profiles for RAD IV

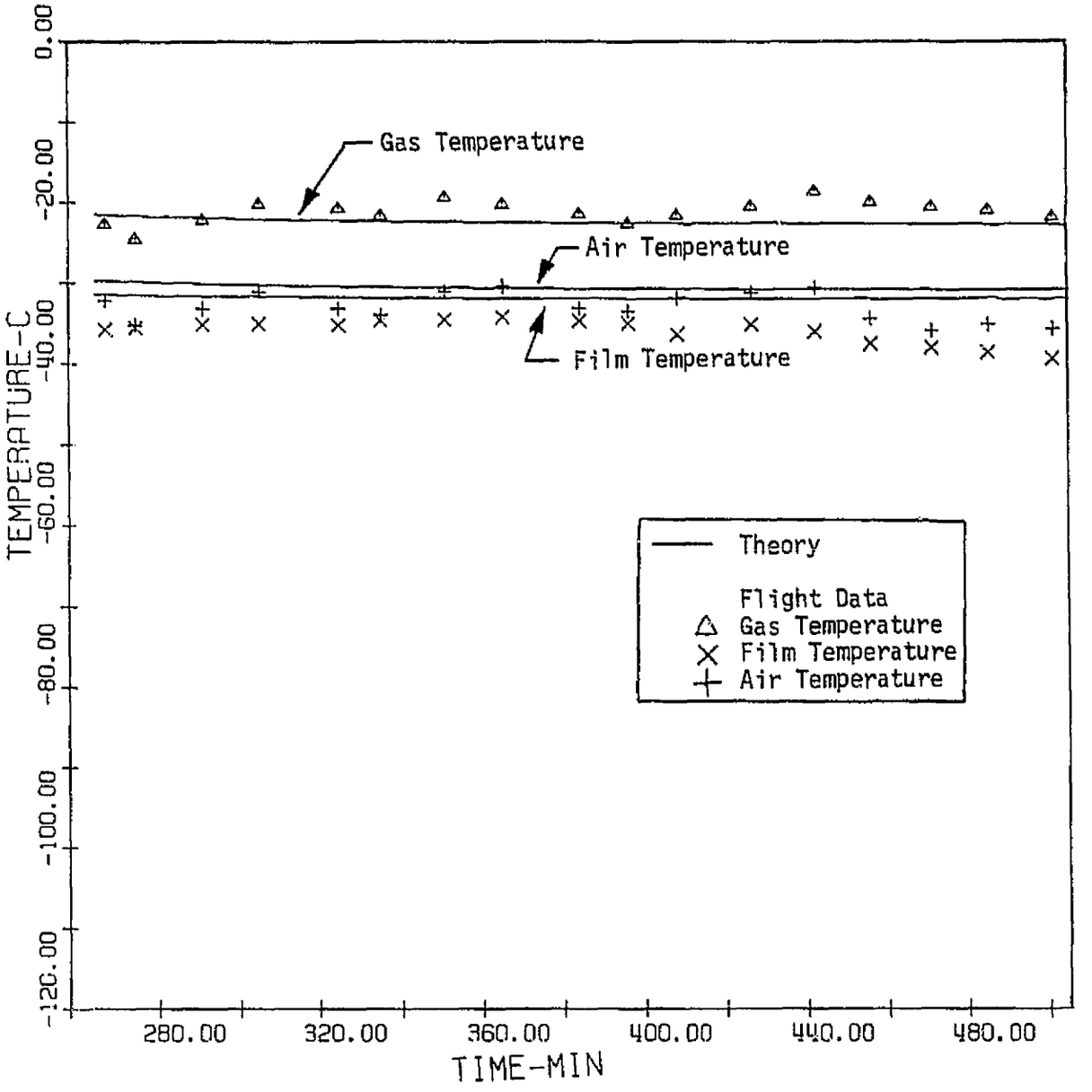

Figure 15(b) -- Temperature Profiles for RAD IV

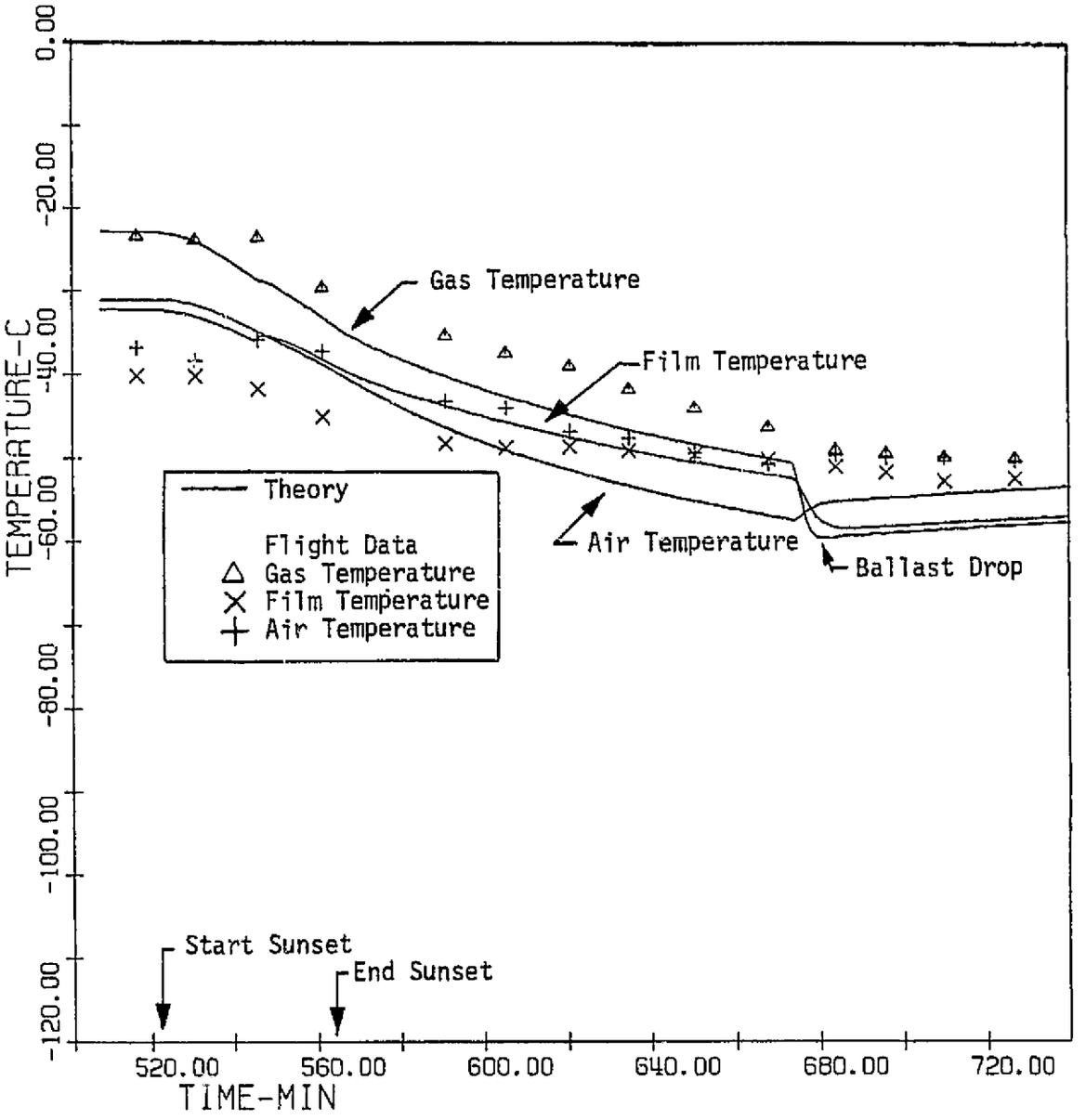

Figure 15(c) -- Temperature Profiles for RAD IV

on Figure 16(a), the resultant pressure trajectory is in good agreement with flight data up to the tropopause. Above this altitude, however, the radiatively inactive model is in serious error and significantly mispredicts the time to float. In addition, as shown on Figure 16(b), the old type of thermal model completely misses the actual flight behavior during and after sunset. This absence of an altitude decrease is due to the fact that the solar absorptivity of polyethylene is very small and that, thus, it is relatively insensitive to the presence or absence of sunlight.

Temperature profiles for the radiatively inactive case are portrayed on Figures 17(a) and 17(b), and they also show very poor agreement with the flight data. During daytime float, the gas and film temperatures predicted by this old approach are on the order of 20°C too cold, and the variation during sunset is not even close to the actual behavior.

Based upon comparison of Figs. 14(a,c) with Figs. 16(a,b) and Figs. 15(a,c) with Figs. 17(a,b), it is obvious that the present model is a significant improvement over previous formulations. In addition, based upon the results of this section and in particular those for RAD IV, it is believed that the present method and code is a valid model for high altitude balloon flight. It should, with correct usage, yield accurate thermal and trajectory information suitable for analyzing and predicting the behavior of scientific balloons.

VI. SUMMARY AND RECOMMENDATIONS

Initially, this research program was formulated around ten tasks. In this section, each task will be briefly discussed and an indication made as to what has and has not been accomplished. Subsequently, suggestions for future work in this area will be stated.

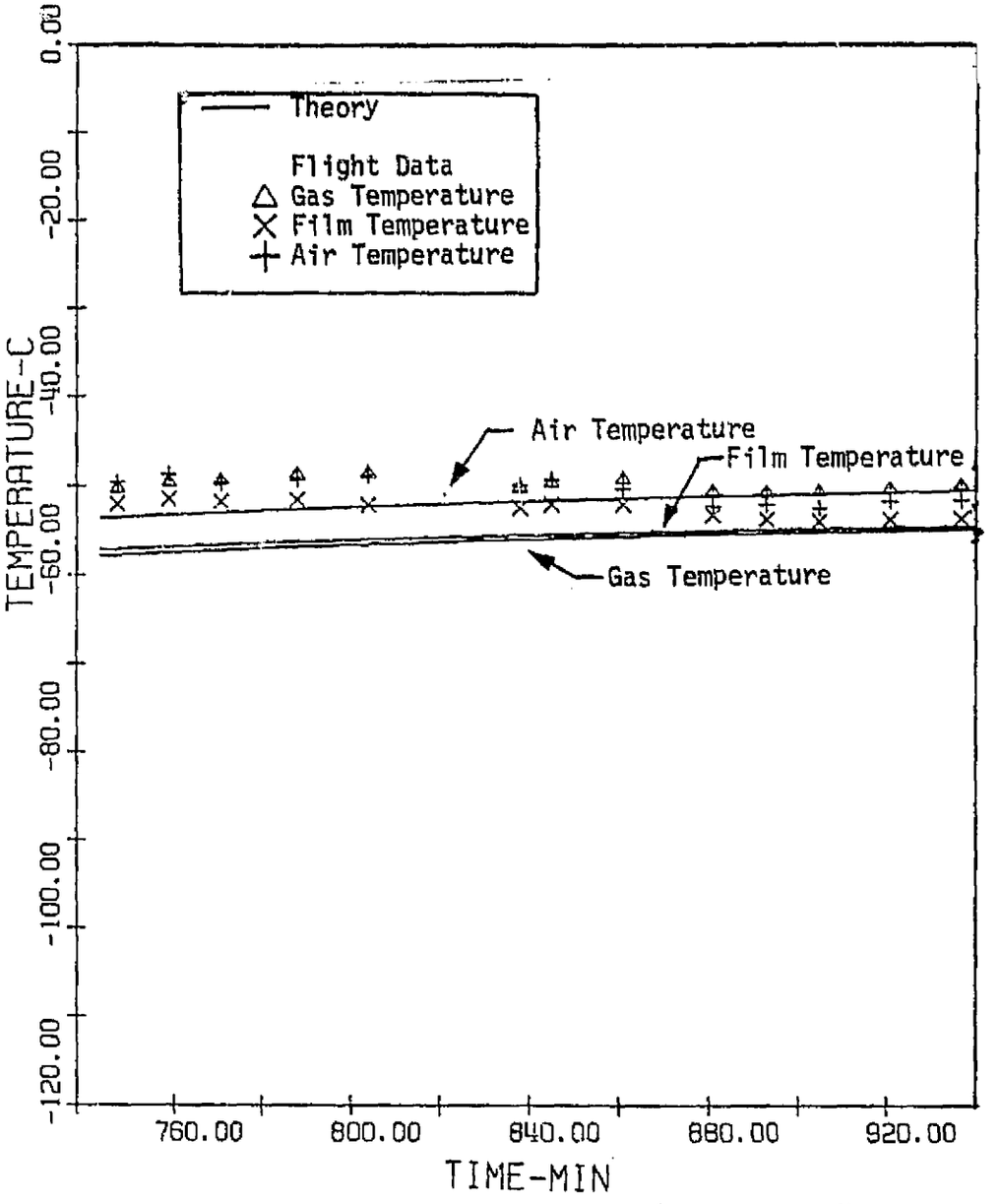

Figure 15(d) -- Temperature Profiles for RAD IV

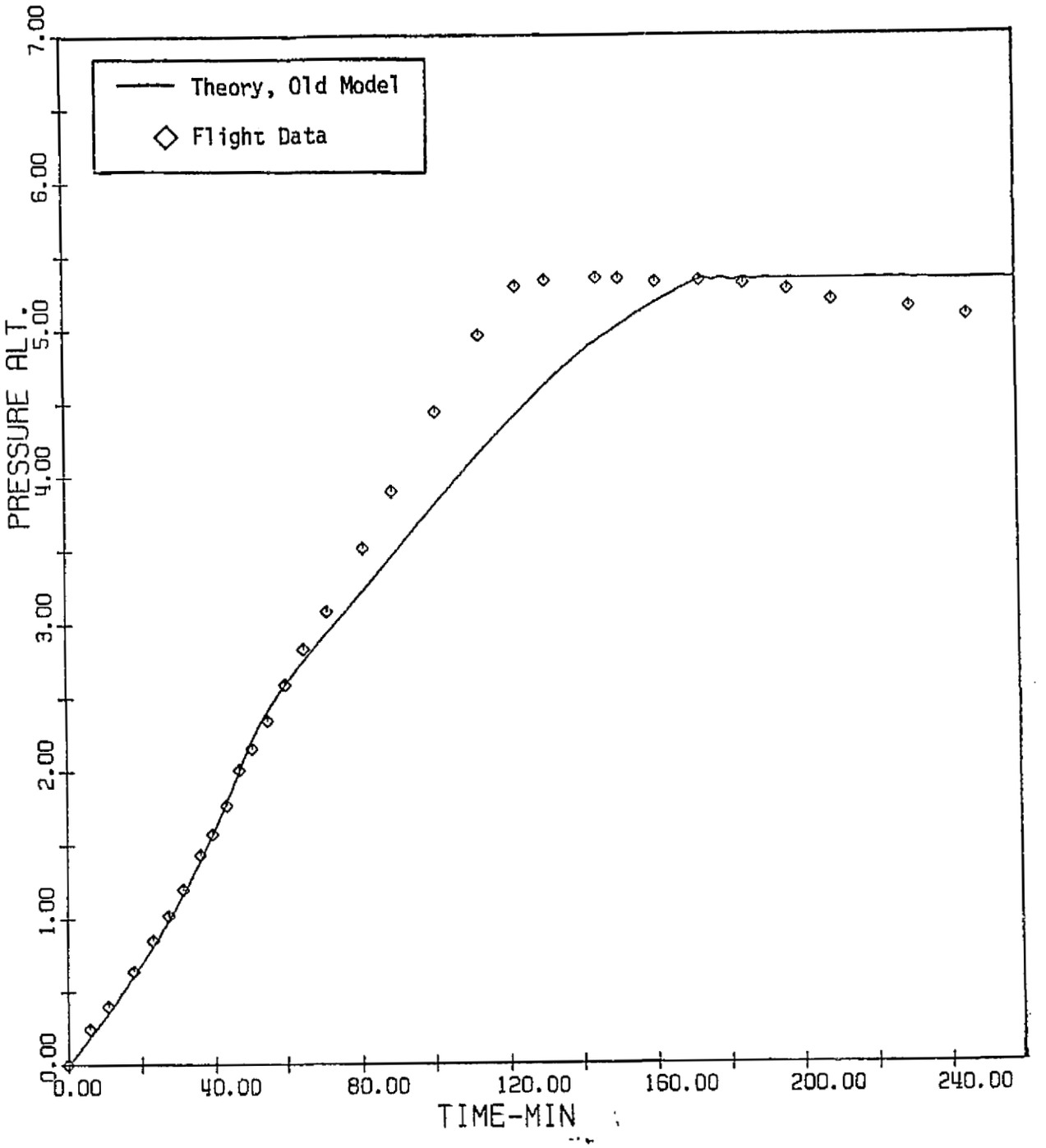

Figure 16(a) -- Pressure Altitude Trajectory for RAD IV

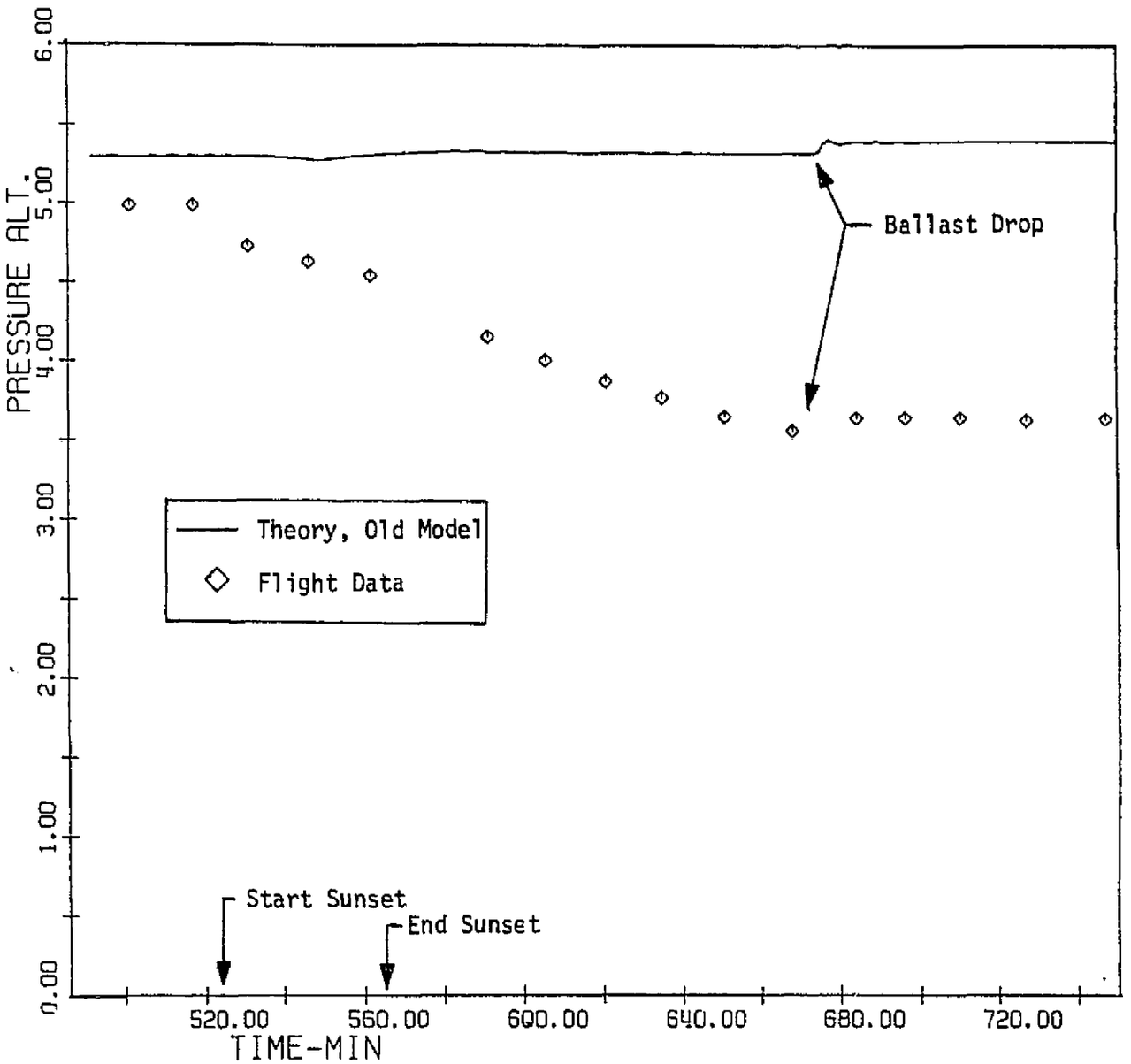

Figure 16(b) -- Pressure Altitude Trajectory for RAD IV

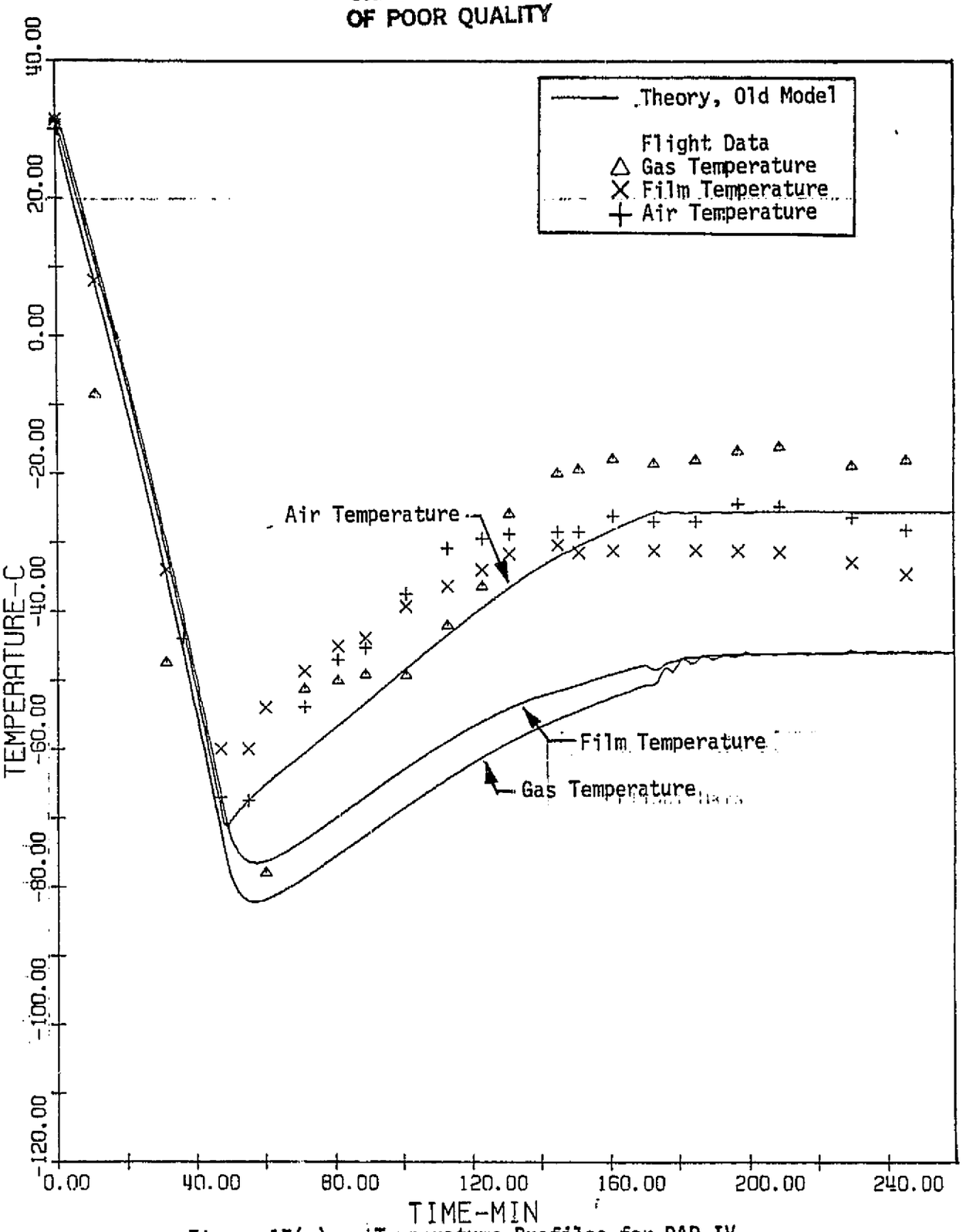

Figure 17(a) -- Temperature Profiles for RAD IV

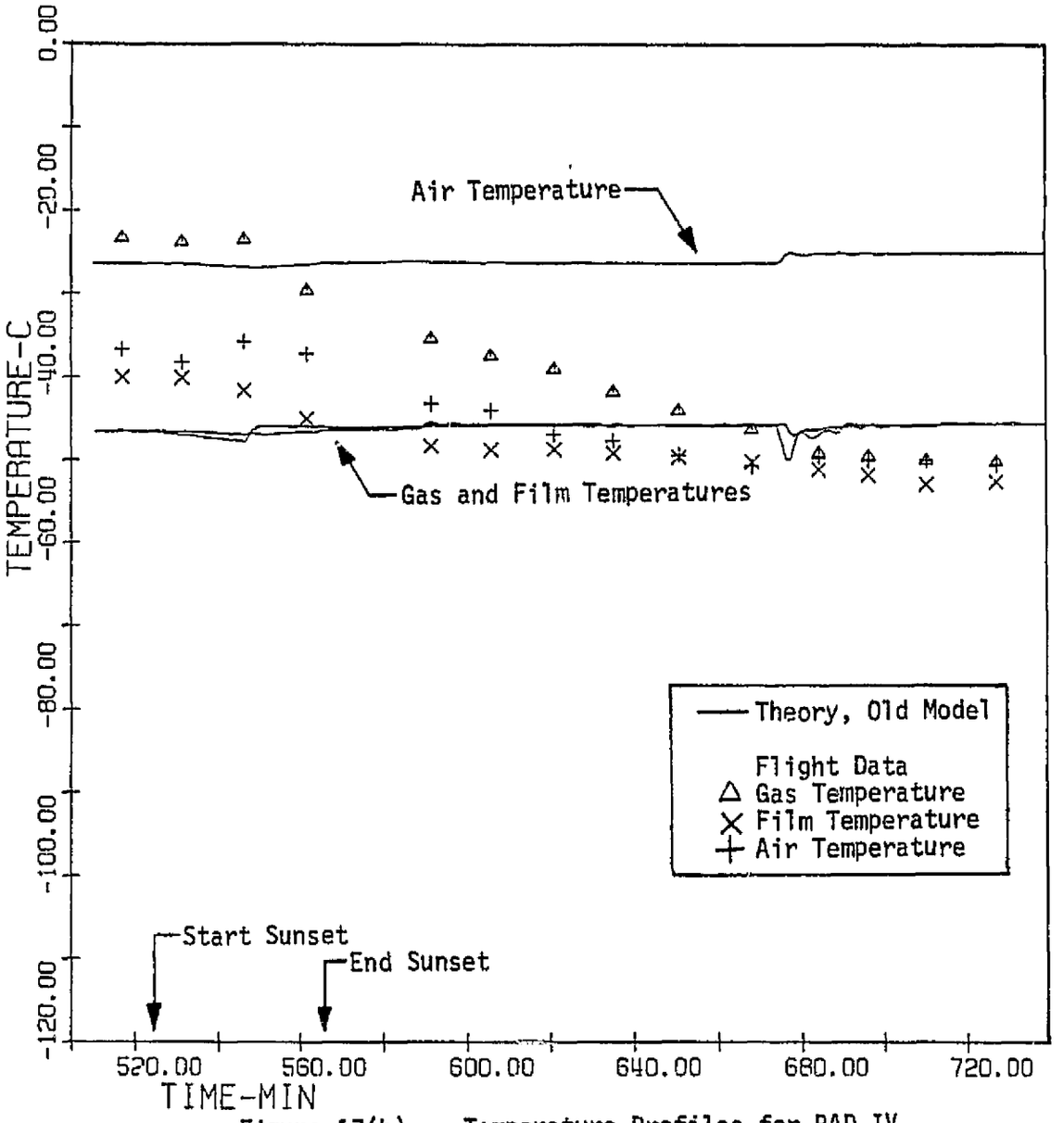

Figure 17(b) -- Temperature Profiles for RAD IV

A. Discussion of Project Tasks

Task 1 - Acquisition of Balloon Film Radiative Property Data

The radiative properties of polyethylene balloon film were, at the request of TAMU, measured by NASA Langley and the data sent to TAMU. This data was subsequently analyzed and incorporated into the present model and program. The acquisition of this information was very significant and served as a major contribution to the success of the present project. If new films are developed for balloon use, they should also be measured in a similar manner, since correct radiative properties are essential for accurate thermal predictions.

Task 2 - Balloon Model Thermal Development

The equilibrium float thermal model, originally developed for NSBF, was extended into a time dependent form as discussed in Section III(A). This model was subsequently initially programmed into a pilot code using a specified balloon trajectory. After a review of the possibilities, it was concluded that the most likely explanation for the observed gas thermal behavior was water vapor contamination, although there is no direct proof. Consequently, the gas absorptivity was deduced from the equilibrium float model, and its emissivity was estimated from water vapor radiation theory. This approach is discussed in Section III(B).

The original objective was to develop a model capable of predicting temperatures within $\pm 1°K$. While the present thermal model is theoretically capable of such accuracy by itself, input data, particularly earth-air IR and cloud effects are not known sufficiently accurately to achieve this goal. Currently, it is believed that in typical applications the present model is accurate within $\pm 2°K$, which is within the error band of current instrumentation techniques.

Task 3 - Trajectory Analysis/Prediction Program

Originally, it was intended to utilize the computer code of Ref. 4 for the basic trajectory program and to incorporate into it a new thermal model. However, as experience was gained with this program, it became obvious that its structure and organization were not user oriented or amenable to straightforward adaptation. Consequently, it was abandoned; and a new code incorporating the new thermal model was developed.[1]

Originally, it had also been planned to perform a systematic sensitivity study and to determine quantitatively the effect of each major parameter and correlation on results. Due to unforeseen problems in the development of the trajectory code, this study was not carried out in the detail originally intended. However, studies were conducted to determine the most important parameters and to develop suitable values and correlations. This action was discussed in detail in Section III. Briefly, it was determined that drag coefficients strongly affect trajectories below the tropopause, that the mass of gas strongly affects performance above the tropopause, and that forced convection significantly affects large volume balloons. In all cases, it was found that the blackball temperature variation, which characterizes the earth-air infrared radiation, is very important.

Task 4 - Flight Test Planning Assistance

Initially, it was proposed that multiple flight tests be conducted by NASA Wallops with the advice and assistance of TAMU. These multiple tests were not actually flown for several reasons. First, it was determined that there was a large amount of data already available in sufficient detail to satisfy the needs and time available of the present investigators. However, the present investigators did discuss with and advise the National Scientific

Balloon Facility Engineering Department on instrumentation and flight profile requirements for such flights. These discussions led to the very successful RAD IV engineering test flight. The results of this flight are discussed in Section V.

Task 5 - Integration of Thermal and Trajectory Models

This task was accomplished and led to the model discussed in Section III and the program described in Ref. (1). Typical results were presented in Section V.

Task 6 - Prediction of Flight Test Results

No flights were actually predicted prior to flight as part of this effort. However, flight 167N or RAD IV was treated in this manner using the fully developed code. Initial prediction yielded good results but led to the discovery of the importance of high cirrus clouds. When the latter were included, the excellent results presented in Section V were obtained.

Task 7 - Analysis of Flight Tests and Comparison with Prediction

The flights of RAD I (913PT), RAD III (979PT), and 1116PT were primarily used for this task. Comparison with flight data led to significant improvements in input specifications, drag coefficient correlations, and heat transfer coefficient formulations.

Tasks 8-9 - Initial and Final Verification

Initial verification was primarily achieved in Task 7 and with studies of Flight 1131 P. RAD IV or flight 167 N was used for final verification; and a comparison of results obtained using the present mode, as opposed to previous models, indicate that the present program is a significant improvement. It is believed that accuracies of ±2°K and trajectories compatible with this variation are possible with the present model/

Task 10 - Final Report and Program

This report and Ref. (1) constitute the accomplishments of this task.

B. Recommendations for Future Work

Based upon the present study, eight areas requiring further investigation have been determined. These suggestions are as follows:

(1) Flight Data Comparisons

Results obtained with the present method and code should be compared to as much flight data as possible. While there exists data in addition to that described in this report, lack of time and insufficient funds prevented its analysis and inclusion; and much of it only contain trajectory information. Accurate and reliable temperature data, including weather and earth-air infrared data, is needed to determine the validity of the present method since the problem is primarily temperature dominated. With only trajectory data, there always exists the possibility of disagreement between theory and flight with no indication as to the cause. Consequently, several flights similar to RAD IV should be conducted and analyzed, and if possible these flights should obtain data over clear and overcast skies. In addition, possibly in a piggy-back mode, some thermal and trajectory data should be obtained for medium size balloons in the 425,000m^3 to 850,000m^3 range. It is believed that such a comparison study will more accurately determine the applicability, strengths, and weaknesses of the present model and determine specifically those types of balloons and flights for which it is adequate.

(2) Detailed Sensitivity Studies

While considerable effort was expended in the present investigation in determining the importance of various quantities, it is believed that the overall understanding of the problem could be significantly enhanced by a detailed sensitivity study. It is suggested that all input parameters and model correlations (i.e. heat transfer, drag, etc.) each be systematically varied by some fixed amount, say $\pm$ 10%, to determine the effect on the overall solution. In this manner, the important variables and correlations would

be detected; and those requiring further study and definition could be determined.

(3) Entrance into Float

Examination of the present results indicates that there is frequently slight disagreement during the approach and entrance to float between theory and flight data. While this discrepancy could be due to the transition from forced to natural convection or to high altitude variations in the blackball profile, its exact origin is unknown. Thus, this area needs and requires further study.

(4) Three Dimensional Model

The present model currently uses average temperature for the balloon film and lifting gas. In actuality, it is known that these temperatures vary slightly with position and sometimes lead to the formation of apparent convection cells. Sometime in the future, a three dimensional thermal model that allows such variations should be developed. Such a model would improve the overall understanding of balloon thermal behavior and possibly lead to a better explanation of observed flight data. It is suggested that initially such a model assume that the lifting gas is radiatively inactive.

(5) Contaminant Determination

In the present study, it has been postulated that the observed lifting gas behavior is due to the presence of a radiatively active contaminant. However, no direct proof of its existence or exact determination of its nature and origin has been obtained. Thus, this possibility needs to be further investigated. It is suggested that a gas sample be taken inside the balloon during daylight float conditions and returned for analysis. A mass spectroscopy analysis of this sample should reveal the existence of a contaminant.

(6) Wind Tunnel and Analytical Drag Studies

As discussed in Section III(D), the effective drag coefficients of balloons appears to be different from that of spheres; and little if any experimental data on balloon shapes exists. Thus, it is suggested that a combined experimental and analytical program be carried out to determine the drag and flow characteristics of balloons. The experimental effort should be wind tunnel tests using models having realistic balloon shapes and should be conducted at Reynolds numbers typical of those encountered in flight. The analytical portion could utilize inviscid axisymmetric numerical methods combined with a laminar-turbulent boundary layer scheme to properly include the effects of viscous interaction and separation in an iterative fashion. Such a combined analytical and experimental program has the potential of providing realistic aerodynamic coefficient and flowfield information.

(7) Earth-air Infrared Data

The present study has revealed that balloon performance is quite sensitive to infrared radiation, as characterized by the blackball temperature. It is suggested that flight data be obtained and subsequently analyzed to more accurately determine the correlation between blackball temperature and weather, time of year, cloud types, and ground cover. In addition, since blackball measurements cannot currently be conducted during the daylight portions of a flight, a correlation between blackball and net radiometer data needs to be obtained for both day and night condition.

(8) Ballasting Studies

Finally, the present method and code offers an excellent vehicle for studying the effects of ballasting on balloon flight. Frequently, in the present study, the effects of ballasting were observed to range from significant to inconsequential. Thus, a systematic study of ballasting effects on

balloon behavior would be desirable. In particular, it would be desirable to configure the present code into a form which would determine the ballasting schedule required for a specific balloon performance. In addition, both the present and reconfigured code, should be used to determine optimum ballasting procedures for such events as sunset, etc.

VII. CONCLUSION

It is believed that the present project has yielded a theoretical model and computer program that will permit better predictions of balloon temperatures and trajectories and which will lead to a better understanding of overall balloon behavior. Such predictions and analyses can be used to provide better input data for advanced structural analysis methods and for studies of ballast management and balloon performance optimization.

VIII. ACKNOWLEDGEMENTS

This research was primarily supported by the National Aeronautics and Space Administration, Wallops Flight Center, Wallops Island, VA under Contract NAS6-3072. The technical monitor for this work was Mr. Harvey Needleman of the Balloon and Lighter than Air Section, Sounding Rocket and Balloon Program Branch, of NASA Wallops Flight Center. Partial support in the form of salaries and computer funds was also provided by the Aerospace Engineering Division of the Texas Engineering Experiment Station.

The authors also wish to express their appreciation to the staff of the NASA Wallops, and to the members of the Engineering Department, National Scientific Balloon Facility, Palestine, Texas for the provision of flight data and their helpful discussions and advice. In addition, we would also like to thank L.G. Clark and C.C. Riser of NASA Langley for providing balloon film radiative property data.

IX. REFERENCES

1. Horn, W. J. and Carlson, L. A., "THERMTRAJ: A Fortran Program to Compute the Trajectory and Gas and Film Temperatures of Zero Pressure Balloons," Texas Engineering Experiment Station Report TAMRF-4217-81-02, June 1981.

2. Oakland, L., "Summary Report on Balloon Physics as Related to Long Duration Flights," Winzen Research, Inc., South St. Paul, Minn., August 1963.

3. Germeles, A. E., "Vertical Motion of High Altitude Balloons," Tech. Report No. 4, Prepared for Office of Naval Research by A. D. Little, Inc., Cambrige, Mass., 1966.

4. Kreith, F. and Kreider, J. F., "Numerical Prediction of the Performance of High Altitude Balloons," NCAR Tech. Note NCAR-IN/STR-65, February 1974.

5. Nelson, J. R., "Criteria For Controlling Vertical Motion of Stratospheric Balloons, "Winzen Research, Inc. Report No. N00014-75-C-0072-04, WRI, Inc., South St. Paul, Minn., November 1975.

6. Nishimura, J., Fujii, M., and Yamagami, T., "Effect of Heat Transfer on the Motion of a Balloon at High Altitudes," Tokyo University Institute of Space and Aeronautical Science: Bulletin. Vo. 9(1B), pp. 167-185, 1973.

7. Kreider, J. F. , "Mathematical Modeling of High Altitude Balloon Performance," AIAA Paper No. 75-1385, 1975.

8. Lucas, R. M. and Hall, G. H., "The Measurement of High Altitude Balloon Gas Temperature," Proc. 4th AFCRL Scientific Balloon Symposium, J. F. Dwyer, Ed., AFCRL-67-0075, pp. 279-293, 1967.

9. Lucas, R. M. and Hall, G. H., "The Measurement of Balloon Flight Temperatures through Sunset and Sunrise," Proc. 5th AFCRL Scientific Balloon Symposium, AFCRL-68-0661, pp. 121-130, 1968.

10. Lucas, R. M., Hall, G. H., and Allen, B. M., "Experimental Balloon Gas and Film Temperatures," Proc. 6th AFCRL Scientific Balloon Symposium, L. A. Grass, Ed., AFGL-70-0543, pp. 227-241, 1970.

11. Carlson, L. A., "A New Thermal Analysis Model for High Altitude Balloons," Proc. 10th AFGL Scientific Balloon Symposium, C. L. Rice, Ed., AFGL-TR-79-0053, pp. 187-206, March 1979.

12. Rotter, J. J., "NSBF Heavy Load Program--Final Report," NSBF, Palestine, Texas, September 1980.

13. Kreith, F., Principles of Heat Transfer, 3rd Ed. Harper & Row, New York, 1973, pp. 219-308.

14. Herzberg, G., Atomic Spectra and Atomic Structure, Dorer, New York, 1944, pp. 64-66.